

# 1 Vertical profiles of volatile organic compounds and fine particles in 2 atmospheric air by using aerial drone with miniaturized samplers and 3 portable devices

4 Eka Dian Pusfitasari<sup>1,2</sup>, Jose Ruiz-Jimenez<sup>1,2</sup>, Alekski Tiusanen<sup>1</sup>, Markus Suuronen<sup>1</sup>, Jesse Haataja<sup>3</sup>, Yusheng  
5 Wu<sup>3</sup>, Juha Kangasluoma<sup>3</sup>, Krista Luoma<sup>3,4</sup>, Tuukka Petäjä<sup>3</sup>, Matti Jussila<sup>1,2</sup>, Kari Hartonen<sup>1,2\*</sup>, and Marja-  
6 Liisa Riekkola<sup>1,2\*</sup>

7 <sup>1</sup>Department of Chemistry, P.O. Box 55, FI-00014 University of Helsinki, Finland

8 <sup>2</sup>Institute for Atmospheric and Earth System Research, Chemistry, Faculty of science, P.O. Box 55, FI-  
9 00014 University of Helsinki, Finland

10 <sup>3</sup>Institute for Atmospheric and Earth System Research, Physics, Faculty of science, P.O. Box 64, FI-00014  
11 University of Helsinki, Finland

12 <sup>4</sup>Finnish Meteorological Institute, P.O. Box 503, FI-00101 Helsinki, Finland

13

14 \*Corresponding authors: Dr. Kari Hartonen (kari.hartonen@helsinki.fi) and prof. Marja-Liisa Riekkola  
15 (marja-liisa.riekkola@helsinki.fi)

16

17 **Abstract.** The increase of volatile organic compounds (VOCs) emissions released into the atmosphere is one  
18 of the main threats to human health and climate. VOCs can adversely affect human life through their  
19 contribution to air pollution directly and indirectly by reacting via several mechanisms in the air to form  
20 secondary organic aerosols. In this study, aerial drone equipped with miniaturized air sampling systems  
21 including up to four solid-phase microextraction (SPME) Arrows and four in-tube extraction (ITEX)  
22 samplers for the collection of VOCs, along with portable devices for the real-time measurement of black  
23 carbon (BC) and total particle numbers at high altitudes was exploited. In total, 135 air samples were collected  
24 under optimal sampling conditions ~~in October 2021~~ from October 4 to October 14, 2021 at the boreal forest  
25 SMEAR II Station, Finland. A total of 48 different VOCs, including nitrogen-containing compounds,  
26 alcohols, aldehydes, ketones, organic acids, and hydrocarbons, were detected at different altitudes from 50  
27 to 400 m above ground level with the concentrations up to 6898 ng m<sup>-3</sup> in gas phase and 8613 ng m<sup>-3</sup> in  
28 particle phase. Clear differences in VOCs distribution were seen in samples collected from different altitudes,  
29 depending on the VOC sources. It was also possible to collect aerosol particles by the filter accessory attached  
30 on the ITEX sampling system, and five dicarboxylic acids were quantified with the concentrations of 0.43 to  
31 10.9 µg m<sup>-3</sup>. The BC and total particle number measurements provided similar diurnal patterns, indicating

32 their correlation. For spatial distribution, ~~surprisingly~~ the BC concentrations were increased at higher  
33 altitudes being 2278 ng m<sup>-3</sup> at 100 m and 3909 ng m<sup>-3</sup> at 400 m. The measurements onboard the drone  
34 provided insights into horizontal and vertical variability in BC and aerosol number concentrations above the  
35 boreal forest.

36 **Keywords:** aerial drone; miniaturized air sampling systems; solid-phase microextraction Arrow; in-tube  
37 extraction; volatile organic compounds; black carbon; total particle number.

## 38 1. Introduction

39 The global phenomenon of climate change has attracted a huge attention in the past decades. Atmospheric  
40 aerosol particles can influence the climate system directly by scattering sunlight, transmission, and absorption  
41 of radiation, and indirectly by acting as nuclei for cloud formation (Hemmilä, 2020; Kim et al., 2017; Oh et  
42 al., 2020). Fine aerosol particles have sizes close to the wavelength range of the visible light, and therefore  
43 they are expected to have a stronger climatic impact than larger particles (Kanakidou et al., 2005). In addition,  
44 the aerosol particles also give an adverse effect on air quality and human health by exposing human's  
45 respiratory system to aerosol particulate matter (PM) that can get into lungs and translocate into vital organs  
46 due to their tiny size (Fu et al., 2013).

47 The formation and growth process of aerosol particles have been studied by many research groups (Ahlberg  
48 et al., 2017; Camredon et al., 2007; Casquero-Vera et al., 2020; Kulmala et al., 2013, 2014; Peng et al., 2021;  
49 Ziemann and Atkinson, 2012). To study the particle formation in the atmosphere, it is important to assess the  
50 possible sources of the atmospheric particles, for instance by the presence of volatile organic compounds  
51 (VOCs). Hydrocarbons and amines e.g. have been extensively investigated either by modelling or by  
52 laboratory chamber experiments to show their contribution to secondary organic aerosol (SOA) formation.  
53 These VOCs, along with other thousands of organic gaseous trace species, are directly emitted from biogenic  
54 and anthropogenic sources. In the atmosphere, VOCs are oxidized by reactions with atmospheric oxidants  
55 such as  $O_3^-$ ,  $OH^-$ ,  $NO_3^-$  and  $Cl^-$  radicals to form less volatile products and further subsequently partition into  
56 aerosol particle leading to SOA formation (Almeida et al., 2013; Kulmala et al., 2014; Zahardis et al., 2008;  
57 Ziemann and Atkinson, 2012). The SOAs then become the major components of fine aerosol particulate  
58 matter, such as PM 10 and PM 2.5 that pollutes the environment (Fermo et al., 2021; Ge et al., 2011; Kulmala  
59 et al., 2014).

60 Another important component that contributes to air pollution is Black Carbon (BC), which is emitted mostly  
61 as a byproduct of fossil fuel combustion and biomass burning (Hyvärinen et al., 2011). In addition, industry,  
62 energy production, and domestic cooking contribute to the BC in the atmosphere (Kumar et al., 2015). BC  
63 has been associated with adverse effects on human health, such as premature mortality, and also on earth  
64 temperature and climate, since it absorbs solar radiation very strongly (Anenberg et al., 2012; Jacobson,  
65 2010).

66 In addition to VOCs and BC, atmospheric organic acids, such as low molecular weight (LMW) dicarboxylic  
67 acids are also recognized as ubiquitous aerosol constituents in the urban region. As highly water-soluble  
68 compounds they have the capability to significantly enhance the hygroscopicity of aerosol particles  
69 (Kanakidou et al., 2005). LMW diacids can be emitted from biomass burning, vehicular exhausts, natural  
70 marine, and also produced from the atmospheric photo-oxidation of various organic precursors (Fu et al.,  
71 2013; Kawamura and Sakaguchi, 1999; Rinaldi et al., 2011).

72 The condensation particle counters (CPC) are important devices for the measurement of aerosol number  
73 concentrations and aerosol particle fluxes (McMurry, 2000; Kangasluoma and Attoui, 2019; Petäjä et al.,  
74 2001). CPCs are commonly used in the ambient air quality monitoring to measure the number concentration  
75 of airborne submicron particles with sizes down to a few nanometers (Asbach et al., 2017; Buzorius et al.,  
76 1998). The conventional CPCs have generally not been used as portable devices due to their weight and size.  
77 However, recently small CPCs are emerging and being deployed for example for vertical profiling on-board  
78 drones (Kim et al., 2018; Carnerero et al., 2018), and other platforms (Petäjä et al., 2012).

79 In our previous research, we used reliable and versatile miniaturized air sampling (MAS) techniques, which  
80 have many benefits for on-site sampling, such as small size, low sampling time, environmental friendliness,  
81 easy operation and flexibility for practical applications and automation (Lan et al., 2020; Pusfitasari et al.,  
82 2022; Ruiz-Jimenez et al., 2019). Solid-phase microextraction (SPME) Arrow and in-tube extraction (ITEX)  
83 sampling systems have been successfully employed for the reliable collection of VOCs from ambient air  
84 samples (Lan et al., 2019b, a; Pusfitasari et al., 2022). An exhaustive sampling technique ITEX sampling  
85 system with large sorbent volume can be fully automated, and it provides continuous air sampling, reliable  
86 analysis, and quantification (Lan et al., 2019a; Pusfitasari et al., 2022). As an active sampler, ITEX system  
87 allows the simultaneous collection of gas and particle phase compounds. Extra sampling accessories,  
88 including adsorbent trap and filter accessories together with ITEX have enhanced the selectivity of the  
89 sampling system and allowed the ITEX to collect only gas phase (Pusfitasari et al., 2022). After sample

90 collection, the compounds were desorbed from the samplers, separated and detected by thermal desorption  
91 (TD) gas chromatography-mass spectrometry (GC-MS).

92 In this study, the sampling of VOCs and measurement of total particle number concentration and Black  
93 Carbon (BC) directly at various altitudes, from 50 to 400 m, were performed using an aerial drone as the  
94 platform as in our previous research (Lan et al., 2021; Pusfitasari et al., 2022; Ruiz-Jimenez et al., 2019). The  
95 sampling platform contained now up to four SPME Arrows and four ITEX units, with additional portable  
96 commercial BC device for BC real-time measurement and a lab-made portable CPC for total particle number  
97 observation. The compositions of different gas phase fractions collected both by SPME Arrow and ITEX  
98 systems, aerosol particles collected by ITEX sampling including filter accessory as well as BC and particle  
99 numbers were evaluated at different altitudes and temporal variation at boreal forest SMEAR II Station in  
100 October 2021. In addition, the possible correlation between VOCs, BC and total particle number  
101 concentrations were also clarified.

## 102 **2. Materials and methods**

### 103 **2.1. Reagent and materials**

104 Detailed information of reagents used, including their purities, is given in the supplemental information S1.

105 Empty ITEX units, DVB-PDMS and Carbon coated WR-SPME Arrow systems were purchased from BGB  
106 Analytik AG (Zurich, Switzerland). TENAX-GR was purchased from Altech (Deerfield, IL, USA). The  
107 mesoporous silica-based materials, the Mobil Composition of Matter No. 41 (MCM-41) and titanium  
108 hydrogen phosphate-modified (MCM-41-TP) materials were synthesized via sol-gel template as described  
109 in our previous publication (Lan et al., 2019a). The instructions for ITEX packing with 30 mg MCM-41-TP  
110 and 60 mg Tenax-GR are described in Lan *et al.* (2019b). The preparation of MCM-41-SPME Arrow with  
111 the sorbent thickness of 40  $\mu\text{m}$  and length of 20 mm, is found from Lan *et al.* (2019a).

### 112 **2.2. Instrumentation**

113 A lab-made permeation system was employed to create an artificial gas-phase sample in the laboratory (Lan  
114 et al., 2019a, 2021; Pusfitasari et al., 2022). A PAL Cycle Composer and PAL RTC autosampler that were  
115 used for sample collection and desorption in the laboratory were from CTC Analytics (Zwingen,  
116 Switzerland). An Agilent 6890N gas chromatograph coupled with an Agilent 5975C mass spectrometer  
117 (Agilent Technologies, Pittsburg, PA, USA) was used for the method optimization and quality assurance tests  
118 for air samples in the laboratory. For onsite analysis, an Agilent 6890 N gas chromatograph (Agilent  
119 Technologies, Pittsburg, PA, USA) equipped with a lab made ITEX heater for thermal desorption was

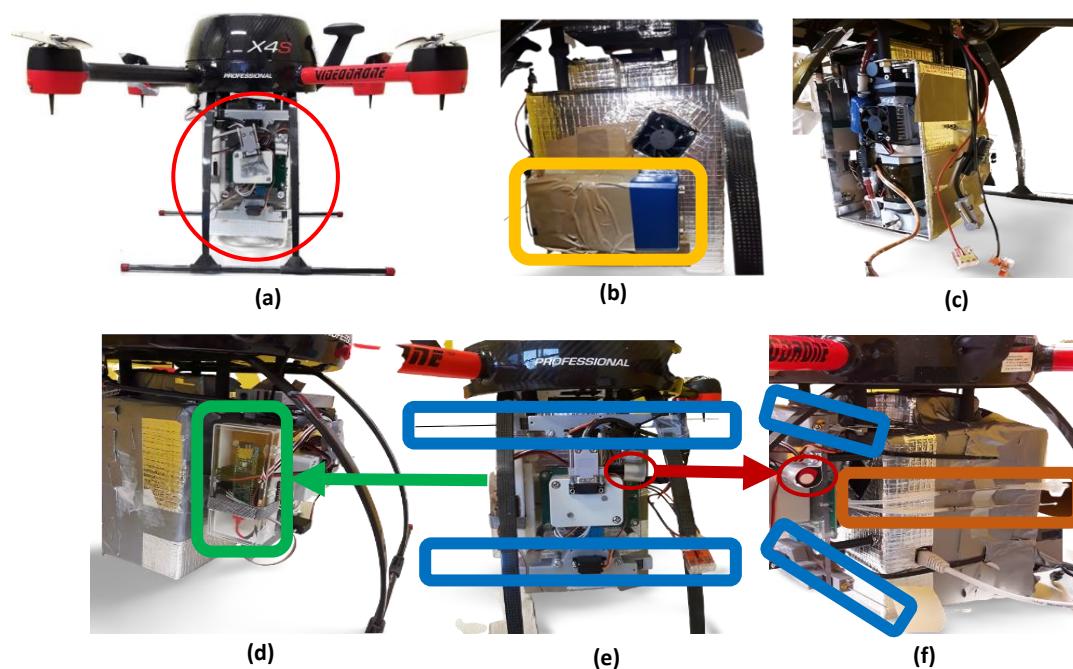
120 employed and coupled to an Agilent 5973 mass spectrometer. The GC capillary column used for the  
121 chromatographic separations was an InertCap™ for amines (30 m length x 0.25 mm i.d., without any  
122 information for the film thickness, GL Sciences, Tokyo, Japan).

123 For organic acid determination, an Agilent 1260 Infinity high performance liquid chromatography (HPLC)  
124 system equipped with a binary pump, autosampler, degassing unit, and a column compartment was employed  
125 and coupled to an Agilent 6420 triple-quadrupole mass spectrometer with electrospray ion source (ESI)  
126 (Agilent Technologies, Palo Alto, CA, USA). Chromatographic separations were performed with a 2.1x150  
127 mm SeQuant® ZIC®-cHILIC (3 µm particle size) hydrophilic interaction liquid chromatography (HILIC)  
128 column (MerckKGaA, Darmstadt, Germany). A KrudKatcher ULTRA HPLC in-line filter (0.5 µm) from  
129 Phenomenex Inc (Torrance, CA, USA) protected the column from particulate impurities.

### 130 2.3. Drone platform construction

131 A remote-controlled Geodrone X4L (Videodrone, Finland), similar to that used in our previous studies (Lan  
132 et al., 2021; Pusfitasari et al., 2022) with some modifications, was employed to carry out miniaturized air  
133 sampling and analysis systems. With the dimension of 58x58x37 cm (width x depth x height), it could carry  
134 the modified sampling box including our MAS system (up to four SPME Arrow units and up to four ITEXs)  
135 with a new, light sampling pump for ITEX system. In addition, some portable devices were also attached to  
136 the drone to measure Black Carbon (BC) and particle sizes by condensation particle counter (CPC). BC  
137 portable device in the field was an AethLabs AE51-S6-1408, with the application version of 2.2.4.0 (San  
138 Francisco, CA, USA). It was operated at 880 nm wavelength, with the air flowrate of 99 mL/min. The  
139 portable CPC was a laboratory-made. The portable CPC measured total aerosol particle number concentration  
140 between sizes from 20 nm and 5 µm. The references for BC and particle concentrations were measured at  
141 Boreal forest SMEAR II Station at the altitude of 4 meters by an AE33 (operated at 880 nm) and an aerosol  
142 electrometer (TSI 3772), respectively.

143



144

145 **Figure 1.** Drone platform sampling system with: (a) Air sampling box carried by aerial drone. (b) BC placed  
 146 behind the box. (c) CPC inserted into the sampling box. (d) The right side of the sampling box is a sensor  
 147 that measured temperature and relative humidity. (e) Front position of the sampling box consisted of SPME  
 148 Arrow units (marked with blue) and a VOC sensor (red circle). (f) Sides of the sampling box included ITEX  
 149 unit and filter accessory (brown).

#### 150 2.4. Gas chromatography-mass spectrometry analysis

151 The SPME Arrow and ITEX sampling systems were preconditioned at 250 °C for 10 min under inert gas N<sub>2</sub>.  
 152 Prior to sampling, decafluorobiphenyl vapor (as an internal standard) was spiked to SPME Arrow and ITEX  
 153 for 1 min and 5 mL, respectively. After sampling, the SPME Arrow unit was injected to the GC inlet to  
 154 desorb the analytes at the temperature of 250 °C for 1 min. While for ITEX, 800 μL of He was aspirated to  
 155 the ITEX syringe, and the analytes were desorbed at the temperature of 250°C and injected into the GC-MS  
 156 system by moving the plunger down with the injection speed of 200 μL s<sup>-1</sup>. All the analyses were done in  
 157 splitless injection at 250 °C. For chromatographic separations, the GC oven temperature was programmed  
 158 from 40 °C (held for 2 min) to 250 °C (held for 10 min) at a rate of 20 °C min<sup>-1</sup>. The temperature of transfer  
 159 line, ion source and quadrupole were 250, 230 and 150 °C, respectively. Electron ionization (EI) mode (70  
 160 eV) was used, and the scan range was from m/z 15 to 350. Helium (99.996 %, AGA, Espoo, Finland) was  
 161 used as a carrier gas at a constant flow rate of 1.2 mL min<sup>-1</sup>.

162 **2.5. Hydrophilic Interaction liquid chromatography-tandem mass spectrometry method for organic**  
163 **acids analysis**

164 Acetonitrile (ACN) was used as the main organic solvent containing 0.01 % formic acid (FA) (as Eluent A),  
165 while Eluent B is aqueous 0.01 % FA solution. The applied LC gradient was the following: 5 % B (0-6 min),  
166 5 to 20 % B (5-18 min), and post run for 15 min. The flow rate for the analysis was 0.25 mL min<sup>-1</sup> and column  
167 temperature was maintained at 40 °C. The injection volume was 10 µl. The LC system was coupled to the  
168 triple quadrupole mass spectrometer equipped with ESI. The ion source was operated in both positive and  
169 negative modes.

170 **2.6. Method development, quality control and quality assurance studies.**

171 The optimization study for MCM-41-TP-ITEX system, including optimization of the adsorption and  
172 desorption processes, sampling kinetics, breakthrough volume, and the recovery of the storage time, has been  
173 carried out in our previous study using multivariate analysis (Pusfitasari et al., 2022). The evaluation and  
174 validation of SPME Arrow units coated with MCM-41, DVB-PDMS, and carbon wide range (Carbon WR)  
175 for the sampling of VOCs have also been studied in our previous research (Helin et al., 2015; Lan et al.,  
176 2019b).

177 For TENAX-GR-ITEX sampler, the same method development and validation including the determination  
178 of optimum flow rate, repeatability, reproducibility, and sample storage were done by using our laboratory-  
179 made autosampler. The repeatability and reproducibility of TENAX-GR-ITEX system were studied by  
180 analyzing the model compounds with five different ITEX units five times, each. The sampling flow rate (47  
181 mL min<sup>-1</sup>) was measured at least once for each ITEX during the comparison.

182 The storage study was performed by keeping the TENAX-GR-ITEX system at room temperature and in a  
183 freezer (-20 °C). The purpose was to monitor how conditions affect the adsorption of chemicals in  
184 surrounding environment to TENAX-GR during storage. The retainment of adsorbed analytes in different  
185 conditions was also monitored. The difference in recovery between control sample (not stored) and stored  
186 sample was regarded as the loss of the compound.

187 **2.7. Application, measurement sites and sample collection in the field**

188 The field sampling was carried out at the SMEAR II Station (Station for Measuring Ecosystem–Atmosphere  
189 Relations; (Hari and Kulmala, 2005), with the coordinate of 61.84263° N - 24.29013° E), Hyytiälä, from 4 to

190 14 October 2021. As many as 53 drone flights were performed and 135 air samples in total were collected  
191 (67 samples were collected using ITEX and 68 using SPME Arrow sampling systems). Table 1 shows the  
192 summary of sampling and measurement techniques used in this study.

193 SPME Arrow units with different coating materials, DVB/PDMS, MCM-41, Carbon WR, were exploited to  
194 collect gas phase samples. MCM-41-TP-ITEX and TENAX-GR-ITEX sampling systems were used to  
195 simultaneously collect gas phase and particles. In the field study, the measured ITEX airflow ranged from 40  
196 to 78 mL min<sup>-1</sup>. The flow was carefully measured before the sampling and after analyte desorption. ITEX  
197 sampling volumes were then obtained by multiplying the value of ITEX airflow rate with the sampling time.  
198 Other sampling variables, such as sampling location, remained constant.

199 To study the average composition of VOCs in the atmosphere ([Section 3.3](#)), the samples were collected  
200 simultaneously by ITEX and SPME Arrow systems located on the drone at the altitudes from 50 m to 400  
201 m. Composition samples were collected for 2 min at each altitude and during the descending of the drone by  
202 starting at the highest altitude of 400, followed by 300, 200, 100 and 50 m (Supplemental Fig. S1). In this  
203 case, a total sampling time was 13-14 min (consist of total of 10 min at different altitudes, and 3-4 minutes  
204 when the drone was descending from 400 m to 50 m), with a total flight time close to 20 min including take-  
205 off and landing.

206 The VOC composition at the altitudes of 50 m and 400 m was also separately determined ([Section 3.6](#)). Detail  
207 schematic picture on our sampling system is seen in the Supplemental Fig. S2 (sampling at 50 m for 10 min)  
208 and Supplemental Fig. S3 (sampling at 400 m for 10 min).

209 Evaluation of ITEX sampling with filter accessory was also studied ([Section 3.4](#)). TENAX-GR-ITEX  
210 furnished with filter accessory was employed to collect the gas phase only. A polytetrafluoroethylene (PTFE)  
211 filter with the pore size of 0.2 µm (diameter of 13 mm, VWR) was used as ITEX filter accessory to remove  
212 aerosol particles from the natural air samples. The results obtained were directly compared with those  
213 achieved by Carbon WR-SPME Arrow sampling system. The recovery was calculated from the difference  
214 between concentrations obtained by SPME Arrow and by ITEX furnished with filter accessory. Details about  
215 the experiments, sampling time and altitudes are found from Supplemental Fig. S1.

216 Suitability of particle trap for subsequent analysis was evaluated by the determination of the organic acids  
217 retained or adsorbed in the filter accessory ([Section 3.5](#)). Sample collection from drone at the altitude from  
218 50 to 400 m is seen in Supplemental Fig. S4. Aerosol particles were collected onto the filter attached to ITEX



219 unit in the drone. All the collected samples were wrapped in aluminum foil and placed into separate Minigrip  
220 bags which were stored in freezer (-20 °C) prior to analysis.

221 Portable BC and CPC devices were always active on measuring BC and total particle numbers during the fly  
222 of the drone. The detected BC and total particle numbers obtained with our portable devices were then  
223 compared with those obtained with reference devices at the SMEAR II Station ([Section 3.7](#)).

224 Table 1. Summary of target species, sampling and measurement techniques.

Target species	Sample phase	Sampler	Experiment(s)	Measurement technique
VOCs	Gas phase	ITEX + filter	Section 3.4	GC-MS
VOCs	Gas phase	SPME Arrow	Sec. 3.3; 3.4; and 3.6	GC-MS
VOCs	Particle phase	ITEX	Section 3.3 and 3.6	GC-MS
Carboxylic acids	Particle phase	Filter accessory	Section 3.5	HILIC-MS/MS
Black carbon	Particle phase	Portable AethLabs	Section 3.7	Real-time by Portable AethLabs
Total particle number	Particle phase	Portable CPC	Section 3.7	Real-time portable CPC

225

## 226 2.8. Data Processing and statistical analysis

227 Agilent ChemStation and Agilent Mass Hunter software were exploited for basic data processing, such as  
228 peak identification and integration. An Mzmine2 (version 2.53) software, consisting of an algorithm  
229 Automated Data Analysis Pipeline (ADAP-GC) was used for pre-processing untargeted mass spectrometric  
230 data for detection, deconvolution, and alignment of the chromatographic peaks in natural samples (Ruiz-  
231 Jimenez et al., 2019; Lan et al., 2021; Pusfitasari et al., 2022). NIST2020 (NIST MS Search v.2.3) mass  
232 spectral database was used to check and compare the mass spectra of the aligned peaks as well as their  
233 retention indices. The identified compounds should have a spectral match of >800 and  $\pm 45$  as the maximum  
234 difference between experimental and library Kováts retention indices.

235 Partial least squares regression (PLSR) equations were developed for the quantification and semi-  
236 quantification of the detected compounds in natural air samples (Kopperi et al., 2013; Lan et al., 2021;  
237 Pusfitasari et al., 2022). To develop different PLSR equations for the quantification/semiquantification of  
238 potentially identified compounds, six different concentration levels of 19 detected compounds, i.e. pyridine,  
239 sec-butylamine, 1-butanamine, butanenitrile, 2-propen-1-amine, diethylamine, dimethylformamide,  
240 hexylamine, trimethylamine, nonane, isobutanol, ethylacetate, methyl isobutyl ketone, hexanal, 2,3-

241 butanedione, benzaldehyde, acetophenone, p-cymene and ethyl benzene, were collected and analyzed under  
242 optimal experimental conditions. Afterwards, the data was used for the development of the PLSR equation.

243 Total particle numbers measured by the reference instrument, an aerosol electrometer TSI 3772 at the altitude  
244 of 4 m (ground level), were downloaded directly from the SmartSMEAR open-access database:  
245 <https://smear.avaa.csc.fi/> (Junninen et al., 2009).

246 The measured VOC values that were collected by ITEX sampling system, and BC as well as total particle  
247 numbers at different altitudes were calculated to the same pressure level so that they could be compared to  
248 literature values (Brasseur et al., 1999; Kivekäs et al., 2009; Rajesh and Ramachandran, 2018). In this study,  
249 the reading values were corrected for ambient pressure and temperature as the following:

$$250 \quad A = m_A \left[ \frac{P_0 T}{P T_0} \right]^{-1} \quad (1)$$

251 where A is the corrected value,  $m_a$  is the measured raw concentration,  $P_0$  is the standard atmospheric pressure  
252 (101.3 kPa),  $T_0$  is the standard temperature (293 K), P is the ambient atmospheric pressure, and T is the  
253 ambient temperature. Supplemental Table S1 shows the data at ambient temperatures and pressures used in  
254 this study, as well as the calculated correction factors at different altitudes. In the case of VOC concentrations  
255 collected by SPME Arrows, no correction was applied since the equilibrium constant for current adsorbents  
256 and compounds was not studied at various pressures and temperatures.

### 257 **3. Results and Discussion**

#### 258 **3.1. Optimization of the sampling techniques using gas chromatography-mass spectrometry**

259 The choice of coating materials for SPME Arrow sampling systems was based on the good selectivity of  
260 MCM-41 for nitrogen-containing compounds, suitability of DVB/PDMS for most of the VOCs present in the  
261 air samples, and the capability of Carbon WR to collect volatile compounds, covers a wide range of polarity  
262 and have a good reproducibility (Kim et al., 2020; Lan et al., 2019b; Ruiz-Jimenez et al., 2019). Whereas for  
263 ITEX sampling system, the MCM-41-TP was chosen as a sorbent material since it has proved to have good  
264 selectivity towards nitrogen-containing compounds, while TENAX-GR was selected due to its good  
265 capability to collect different VOCs present in the air (Lan et al., 2019a; Pusfitasari et al., 2022).

266 The optimization containing equilibrium sampling time for SPME Arrow sampling systems, breakthrough  
267 volume for MCM-41-TP-ITEX, desorption temperature and desorption time towards representative

268 compounds such as diethylamine, isobutylamine, triethylamine, trimethylamine, pyridine, p-cymene, 2-  
269 butanol and 2-butanone have been tested in our previous studies (Pusfitasari et al., 2022). Briefly, the average  
270 sampling time that is used before reaching equilibrium for both MCM-41-SPME Arrow and DVB/PDMS-  
271 SPME Arrow units is about 20 min. The cleaning and desorption temperature of 250 °C for 10 min and 1  
272 min, respectively, were selected to be optimal for the conditioning and analysis. The Carbon WR-SPME  
273 Arrow sampling system was also treated in the same way in terms of conditioning and desorption methods.

274 In our previous study, TENAX GR as the sorbent for ITEX's trap-accessory was able to adsorb mostly non-  
275 nitrogen containing compounds and only a small amount of nitrogen containing compounds (Pusfitasari et  
276 al., 2022). In the present study, universal TENAX-GR was used as ITEX sorbent material to collect air  
277 samples. Desorption and conditioning processes were optimized using a previously developed methodology  
278 and optimal conditions similar to MCM-41-TP-ITEX system with selective sorbent (section 2.4). The  
279 repeatability of TENAX-GR-ITEX sampler was also tested, with the RSD between 3.4 and 7.1 %  
280 (Supplemental Tables S2 and S3), whereas the reproducibility between different ITEX units caused also by  
281 ITEX manual packing was between 4 and 18 %.

282 The sampling systems used in this study needed to be stored for a certain period of time before analysis to  
283 accommodate the on-field situation. In our previous study, the sorbent in MCM-41-TP ITEX system could  
284 be stored at -20 °C up to 18 h without losing much of the model compounds, with the recoveries of around  
285 80 % (Pusfitasari et al, 2021). For TENAX-GR sorbent, the recoveries of 98 % were obtained after storage  
286 at -20 °C for 24 h, but only 78 % when the sorbent was stored at room temperature for 24 h. In this study,  
287 the samples collected at the SMEAR II Station had to be analysed after storage of around 2 hours since the  
288 samplers were needed for the upcoming field measurements. Therefore, both MCM-41-TP- and TENAX-  
289 GR-ITEX systems were stored at room temperature only for a few hours before the analysis.

### 290 **3.2. Optimization of organic acid analysis using hydrophilic interaction liquid chromatography** 291 **(HILIC)- tandem mass-spectrometry**

292 HILIC-ESI-MS/MS was employed for analysis of organic acid from filter samples. 18 different acids were  
293 successfully identified and five of them were quantified using the optimized method. For the 18 model acids,  
294 HILIC mobile phase with composition of ACN 80 % (solvent A) and 20 % of 0.005 % FA (solvent B) was  
295 chosen as the best eluent for acids separation (Supplemental Table S4). The second optimized parameter was  
296 drying gas temperature which is important parameter in the ESI technique to allow the eluent from the HILIC

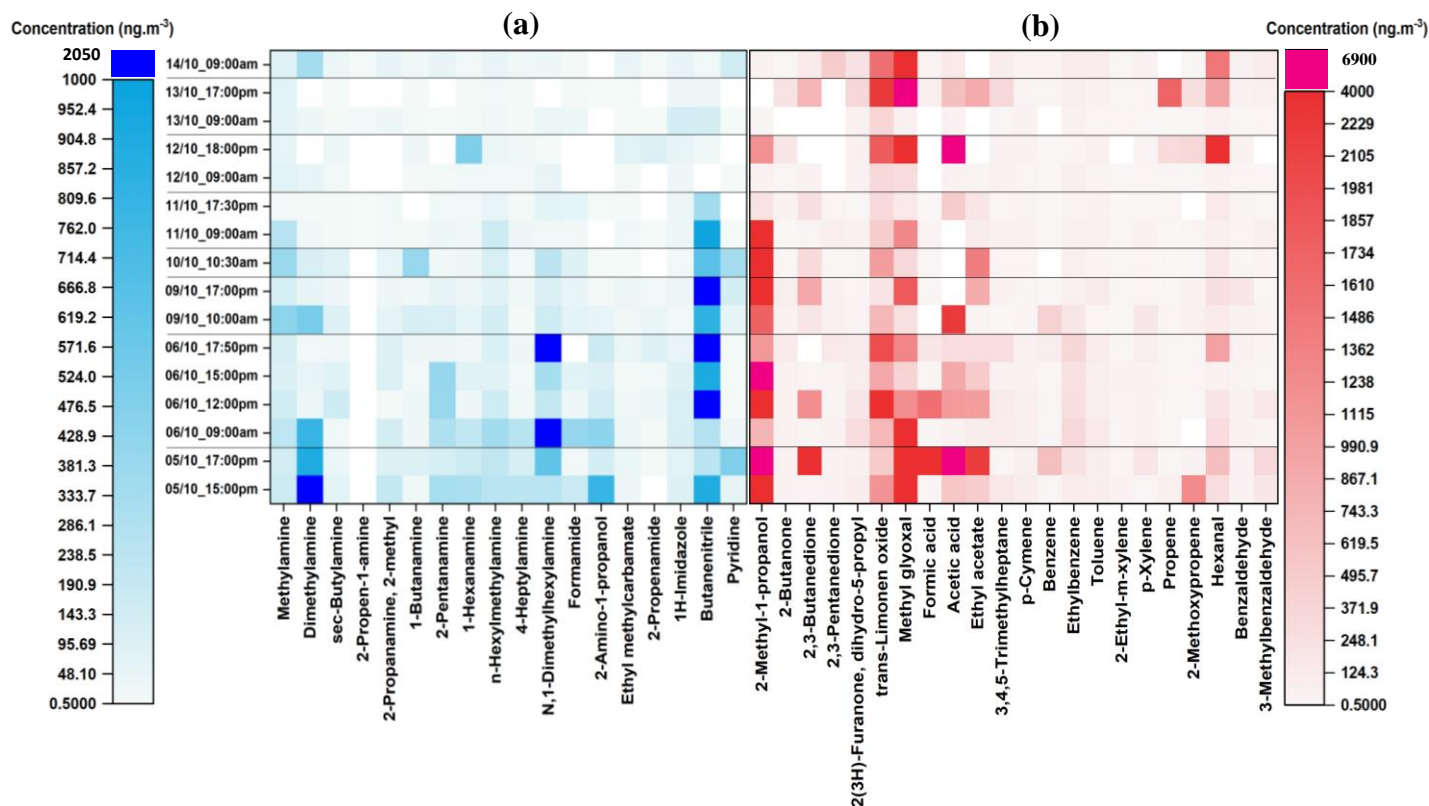
297 column to evaporate as rapidly as possible in the ion source (Kruve, 2016). In this study, using the selected  
298 optimum eluent, i.e. ACN (80 %) and 0.005 % FA (20 %), with the flow rate of 0.25 mL min<sup>-1</sup>, the drying  
299 gas temperature of 275 °C was selected as the optimum temperature. Supplemental Table S5 shows the  
300 established multiple reaction monitoring (MRM) method parameters for each compound using all optimized  
301 parameters including the optimized voltages for other crucial parameters, namely fragmentor voltage,  
302 collision energy and cell acceleration voltage (CAV).

### 303 **3.3.Application of air sampling system at the altitude from 50 to 400 m**

304 In this study, the mesoporous silica-based materials, namely MCM-41 and MCM-41-TP, were used to  
305 selectively collect nitrogen-containing compounds (Lan et al., 2019b; Pusfitasari et al., 2022). Whereas the  
306 commercial universal materials, TENAX-GR and DVB/PDMS were also used to collect other than nitrogen-  
307 containing compounds.

308 MCM-41-TP-ITEX and TENAX-GR-ITEX sampling systems were used to collect atmospheric air samples  
309 containing both gas phase and aerosol particles, while the samples containing only gas-phase were collected  
310 by MCM-41-SPME Arrow and DVB/PDMS-SPME Arrow systems. The concentrations in aerosol particles  
311 were obtained via the subtraction of these results, i.e. MCM-41-TP-ITEX subtracted with MCM-41-SPME  
312 Arrow, and TENAX-GR-ITEX subtracted with the DVB/PDMS-SPME Arrow.

313 Altogether, up to 40 VOCs were detected in gas phase and 48 were in particle phase samples. VOCs with  
314 various functional groups such as nitrogen-containing compounds, alcohols, ketones, aldehydes, small  
315 organic acids, and hydrocarbons were detected both by selective MCM-41 coated SPME Arrow and MCM-  
316 41-TP-ITEX sampling systems and by universal sorbent materials TENAX-GR-ITEX and DVB/PDMS  
317 coated SPME Arrow systems. However, because in our previous study (Lan et al., 2019b; Pusfitasari et al.,  
318 2022), the MCM-41-SPME Arrow and MCM-41-TP-ITEX samplers gave sensitive and reliable results in  
319 collecting selectively nitrogen-compounds, only the results obtained by MCM-41-SPME Arrow and MCM-  
320 41-TP-ITEX samplers are shown for nitrogen-containing compounds in this section. While data for other  
321 VOCs were collected using ITEX with universal sorbent materials TENAX-GR and using DVB/PDMS  
322 coated SPME Arrow.

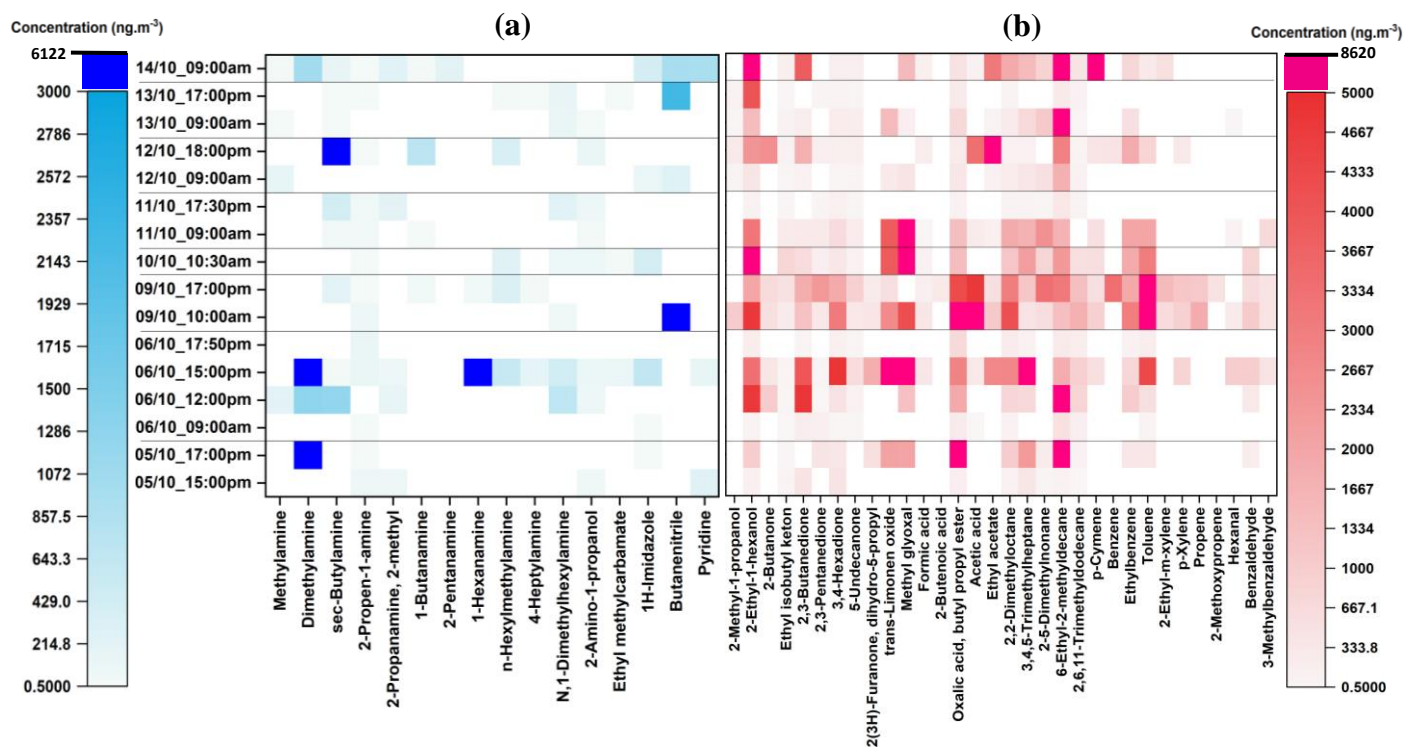


324

325 **Figure 2.** Concentrations of (a) nitrogen-containing compounds and (b) other VOCs in the gas-phase at the  
 326 SMEAR II Station, Hyttiälä at the mixed altitude between 50 and 400 m. (a) Nitrogen-containing compounds  
 327 were collected using MCM-41-SPME Arrow system with selective sorbent, while (b) other VOCs were  
 328 collected using DVB/PDMS-SPME Arrow system with universal sorbent. White color = not detected.

329

330



331

332 **Figure 3.** Concentrations of (a) nitrogen-containing compounds and (b) other VOCs in the particle phase at  
 333 SMEAR II Station, Hyytiälä at the mixed altitude between 50 and 400 m. Samples were collected using  
 334 MCM-41-TP-ITEX system with selective sorbent (a) and TENAX-GR-ITEX systems with universal sorbent  
 335 (b). White color = not detected.

336 As can be seen from Fig. 2, eleven aliphatic amines (methylamine, dimethylamine, sec-butylamine; 2-  
 337 propen-1-amine; 2-methyl-2propanamine; 1-butanamine, 2-pentanamine, 1-hexanamine, n-  
 338 hexylmethylamine, 4-heptylamine, N,1-dimethylhexylamine) and seven other nitrogen-containing  
 339 compounds (formamide, 2-amino-1-propanol, ethylmethylcarbamate, 2-propenamide, 1H-imidazole,  
 340 butanenitrile, and pyridine) were detected, quantified and semi quantified in gas phase samples with the  
 341 concentrations up to 2005 ng m<sup>-3</sup>. While in the particle phase (Fig. 3), the total of 16 nitrogen-containing  
 342 compounds was detected with the concentrations up to 6122 ng m<sup>-3</sup>. These results are comparable to our  
 343 previous study in which the concentrations of nitrogen-containing compounds were up to 2930 ng m<sup>-3</sup> and  
 344 5480 ng m<sup>-3</sup> in gas phase and particle phase, respectively (Pusfitasari et al., 2022). However, the samples  
 345 were collected then at the altitude from 50 to 150 m (Pusfitasari et al., 2022).

346 Dimethylamine, that can be produced by animal husbandry, cattle, landfill, sewage, and also industry (Ge et  
 347 al., 2011), was detected in both gas and particle phase during afternoon with the concentrations up to 1004

348 ng m<sup>-3</sup> for gas phase, and up to 5909 ng m<sup>-3</sup> for the particle phase (Fig. 2a and Fig. 3a). Studies have indicated  
349 that organic amines, including DMA, can be present to large extent in the particles e.g. by transferring from  
350 gas phase to particles (Chen et al., 2022; Zhao et al., 2007; Yu et al., 2017). DMA is one of the most common  
351 and abundant amines found in the atmosphere, and particulate DMA concentrations can increase due to  
352 enhanced BVOC emissions and due to aerosol-phase water that increase their partition to the condensed  
353 phases (Ge et al., 2011; Youn et al., 2015; Chen et al., 2017).

354 Other amines that were detected at high concentrations were methylamine, pentanamine, hexanamine,  
355 hexylmethylamine, and dimethylhexylamine with the concentrations up to 432, 395, 493, 340, and 1393 ng  
356 m<sup>-3</sup>, respectively (Fig. 2a). For the particles, sec-butylamine was detected with the concentrations up to 4090  
357 ng m<sup>-3</sup>, hexanamine up to 4316 ng m<sup>-3</sup> and dimethylhexylamine up to 686 ng m<sup>-3</sup> (Fig. 3a).

358 For nitrogen-containing compounds other than amine, butanenitrile was detected as the highest  
359 concentrations up to 2005 ng m<sup>-3</sup> in gas and 6122 ng m<sup>-3</sup> in particle phases. 2-Amino-1-propanol, pyridine,  
360 and 1-H-imidazole were present in gas phase as the second, third and fourth highest concentrations up to 790,  
361 492, and 136 ng m<sup>-3</sup>, respectively. While in the particle phase, their concentrations were up to 129, 958, and  
362 646 ng m<sup>-3</sup>, respectively. The concentrations of all detected nitrogen-containing compounds at mixed  
363 altitudes can be seen in Supplemental Table S7.

364 For other VOCs, 22 compounds in gas phase (Fig. 2b) and 32 in particle phase (Fig. 3b), containing alcohols,  
365 aldehydes, ketones, small organic acids and hydrocarbons were detected and quantified or semi quantified  
366 with the concentrations up to 6898 ng m<sup>-3</sup> in the gas phase and 8613 ng m<sup>-3</sup> in the particle phase. In the gas  
367 phase, 2-methyl-1-propanol; 2,3-butanedione; trans-limonene oxide, methylglyoxal, acetic acid, ethyl  
368 acetate, and hexanal were discovered almost all the time during the samplings with the concentration up to  
369 4209, 2436, 2210, 4695, 6898, 2198 and 3984 ng m<sup>-3</sup>, respectively (Fig. 2b). While in the particle phase,  
370 almost all detected compounds were present in high concentrations such as 2-ethyl-1-hexanol (4114 ng m<sup>-3</sup>);  
371 2,3-butanedione (4865 ng m<sup>-3</sup>), trans-limonene oxide (6886 ng m<sup>-3</sup>), methylglyoxal (8613 ng m<sup>-3</sup>), aliphatic  
372 hydrocarbons (7091 ng m<sup>-3</sup>), ethyl benzene (3042 ng m<sup>-3</sup>) and toluene (7715 ng m<sup>-3</sup>), (Fig. 3b). Supplemental  
373 Table S8 gives at mixed altitudes (50 to 400 m) the concentrations for all detected VOCs that do not belong  
374 to nitrogen-containing compounds.

375 In the atmosphere, 2,3-Butanedione is naturally occurring in food products such as butter and beers (Boylstein  
376 et al., 2006), while trans-limonene oxide is detected possibly due to the partial oxidation of monoterpene  
377 limonene's olefinic bonds (Hoeben et al., 2012; Karlberg et al., 1992). Methylglyoxal, an important precursor

378 of SOA, is produced in the atmosphere by the oxidation of hydrocarbons, such as isoprene, acetylene, toluene,  
379 and xylenes (Zhang et al., 2016; Fu et al., 2013; Olsen et al., 2007). Other detected compounds, e.g. acetic  
380 acid and ethyl acetate can be released from different sources such as biomass burning and vegetation  
381 (Rosado-Reyes and Francisco, 2006; Khare et al., 1999).

382 The diurnal pattern in both gas and particle-phases was also observed. As can be seen from Fig. 2 in the gas  
383 phase, aliphatic amines that are mostly emitted by biogenic sources were present in lower concentrations in  
384 the evening (started at 17:00 pm) compared to daytime, whereas some amines, namely hexanamine and  
385 dimethylhexylamine, had slightly higher concentrations in the evening. These results agree well with our  
386 previous study in which most of the amines had a diurnal variation with a daytime maximum due to their  
387 dependency on temperature for their emission, indicating the contribution to biogenic sources (Pusfitasari et  
388 al., 2022). High concentrations of some amines in the evenings could be caused by the weak atmospheric  
389 mixing at night resulting in decreased reactions with atmospheric acids (Hemmilä et al., 2018). In contrast,  
390 VOCs that were emitted from other sources had higher concentrations mostly in the afternoons, except for  
391 non-nitrogenated compounds with high concentrations also in the mornings on 11 October 2021. The  
392 anthropogenic sources that might affect this result, were probably carried by the wind from other places and  
393 were mixed in the atmosphere since the samples were collected at high altitudes (up to 400 m). In the particle  
394 phase, there was no clear pattern seen since our samples were mostly collected only in the mornings and late  
395 afternoons. However, in our previous study we found that VOCs had high concentrations in mornings and  
396 evenings since temperature dependency affects the deposition of amines in the colder evenings, and then they  
397 partition back to the atmosphere in the higher temperature mornings (Pusfitasari et al., 2022). In this present  
398 study we can also see from Fig. 3 high concentrations both in the mornings and late afternoons, but  
399 surprisingly also at noon (on 6 October).

400 The correlation among all the VOCs in both gas and particle phases was also studied. R-value close to one  
401 and P-value  $<0.05$  mean that there is correlation between variables. As can be seen from Supplemental Fig.  
402 S5, only a few compounds in gas phase correlate with those detected in the particle phase, such as particulate  
403 benzaldehyde that correlated with alcohol vapors (i.e. gas-phase of 2-methyl-1-propanol and 2-ethyl-1-  
404 hexanol) and some amines (i.e. methylamine, sec-butylamine, 2-pentanamine, and n-hexylmethylamine).  
405 These correlations can be explained by the studies conducted by Perez et al (2017) who was investigating the  
406 implication of aldehyde – amines to the aerosol growth by providing low-energy neutral pathways for the  
407 formation of larger and less volatile compounds (Perez et al., 2017).



408 In addition, we can also see that some nitrogen-containing compounds correlated with aliphatic  
409 hydrocarbons, aliphatic carbonyl, and aliphatic alcohols in the gas phase, indicating that they might be  
410 emitted from the same sources. This finding is supported by the study conducted by Isidorov *et al* (2021).  
411 Although their group could not detect selectively nitrogen-containing compounds because they used  
412 universal sorbent material for the collection of air sample (i.e. DVB/CAR/PDMS-SPME), they could detect  
413 all other VOCs compounds at the same time from the boreal forest (Isidorov et al., 2022).

#### 414 **3.4. Evaluation of ITEX filter accessories**

415 In our previous study, it was proved that a small filter can be used to trap particles allowing only gas phase  
416 enter the ITEX sampler (Pusfitasari et al., 2022; Ruiz-Jimenez et al., 2019). The experiments were properly  
417 designed to check and compare the results achieved for gas phase compounds using a passive SPME Arrow  
418 and an active ITEX + filter sampling systems. In the present study, the samples were collected from 11 to 14  
419 October 2021 and TENAX-GR-ITEX was exploited with the filter accessory. The altitudes for these  
420 experiments were 50-400 m (Supplemental Fig. S1). As can be seen in Supplemental Fig. S6, aliphatic amines  
421 were the major nitrogen-containing compounds detected both in the gas and particle phases. For VOCs  
422 without any nitrogen compounds, following the results in the previous section (i.e. section 3.3.), alcohols,  
423 ketones, aldehydes, organic acids and some hydrocarbons were detected, quantified and semiquantified with  
424 the concentrations shown in Supplemental Fig. S6. The results of the gas-phase sampled by ITEX system  
425 with filter accessory were comparable with the gas phase results obtained by the SMPE Arrow sampling  
426 system.

427 ~~In addition to the comparison of gas phase collected by ITEX (+ filter accessory) and SPME Arrow systems,~~  
428 ~~the recoveries of gas phase obtained by the first sampling system were also evaluated. In addition to the~~  
429 ~~comparison of gas phase collected by ITEX furnished with filter accessory and by SPME Arrow system, the~~  
430 ~~compound recoveries of gas phase obtained by the first sampling system ITEX furnished with filter were also~~  
431 ~~evaluated.~~ The recoveries of non-polar compounds, such as alkanes, were only <50 % (Supplemental Table  
432 S9). The more polar compounds, such as alcohols, acids, and nitrogen-containing compounds, were mostly  
433 detected at higher recoveries from 50 % up to 99 %. Most probably non-polar compounds of the gas phase  
434 were partly adsorbed to the ITEX filter accessory that was made from PTFE (Parshintsev et al., 2011). PTFE  
435 has a non-polar structure due to the distribution of the fluorine atom around the carbon polymer backbone  
436 which balances the electronegative and electropositive charges (Parsons et al., 1992). Hence, our study  
437 proved that ITEX with PTFE filter does not only trap aerosol particles but is also excellent for the collection  
438 of polar compounds, such as nitrogen-containing compounds, of gas phase. Nevertheless, since nitrogen-

439 containing compounds are very water soluble, the humidity level in the air will most likely affect the  
440 distribution of polar compounds between the filter and ITEX adsorbent, e.g. water condensing to the filter at  
441 high humidity.

### 442 3.5. Analysis of aerosol particles collected by ITEX with PTFE filter using liquid chromatography 443 tandem mass spectrometry

444 Filter collecting aerosol particles in ITEX was extracted and analyzed separately by using HILIC-MS/MS to  
445 quantify carboxylic and dicarboxylic acids since most organic acids cannot be analyzed by GC without  
446 derivatization, except small organic acids such as formic acid and acetic acid. The organic acids have  
447 capability to significantly enhance the hygroscopicity of aerosol particles and contribute to the acidity of  
448 precipitation and cloud water.

449 As can be seen in Table 2, five main acids, succinic acid, benzoic acid, phthalic acid, glutaric acid, and adipic  
450 acid, were identified and quantified. Succinic acid was observed almost in every sample and its higher  
451 prevalence could possibly be explained by the fact that it can be formed from common biogenic and  
452 anthropogenic precursors such as isoprene and toluene (Sato et al., 2021). The aromatic acids such as benzoic  
453 acid and phthalic acid were also detected in the samples. The concentrations of benzoic acid (up to  $1.4 \mu\text{g m}^{-3}$ )  
454 were higher than those of phthalic acid (up to  $0.77 \mu\text{g m}^{-3}$ ). Observation of these acids is relevant as their  
455 aromatic hydrocarbon precursors are common in the atmosphere. In addition, phthalic acid has also been  
456 detected in the summer 2012 samples, but then no benzoic acid was detected in the gas phase or particulate  
457 phase (Kristensen et al., 2016).

458 **Table 2.** Concentrations of acids collected from the ITEX filters at the altitudes of 50-400 m.

Sampling time	Succinic acid ( $\text{ng m}^{-3}$ )	Benzoic acid ( $\text{ng m}^{-3}$ )	Phthalic acid ( $\text{ng m}^{-3}$ )	Glutaric acid ( $\text{ng m}^{-3}$ )	Adipic acid ( $\text{ng m}^{-3}$ )
11.10.2021	1416	1416	657	1619	10926
12.10.2021	435-789	1416	769	n.d.	n.d.
13.10.2021	496-4654	n.d.	n.d.	n.d.	n.d.
14.10.2021	n.d.	n.d.	n.d.	1720	6374

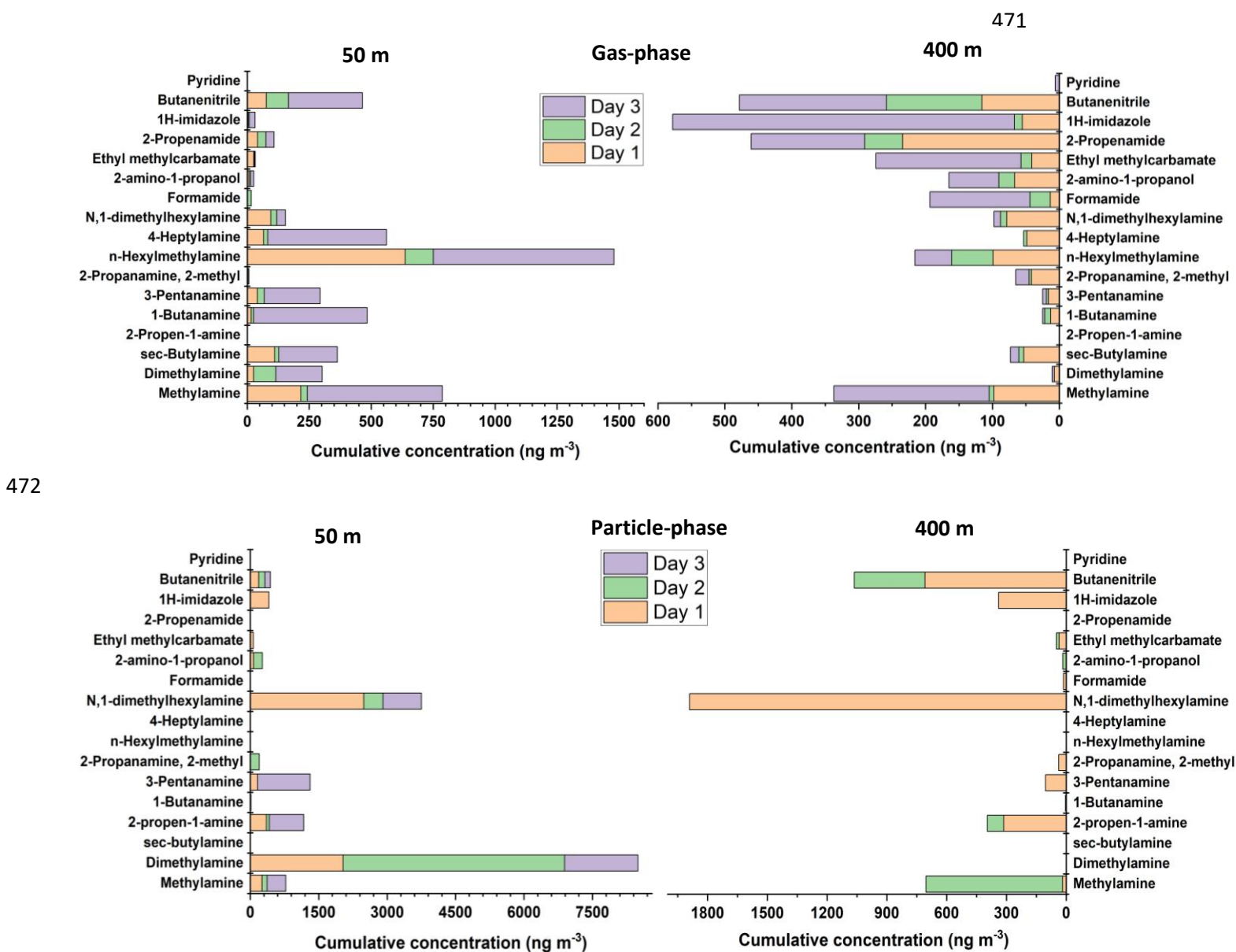
459 \*n.d. = not detected

460 Glutaric and adipic acids were also determined from samples taken on the 11<sup>th</sup> and 14<sup>th</sup> of October. Glutaric  
461 acid and adipic acid have been commonly detected in atmospheric aerosols and cloud droplets (Wen et al.,  
462 2021). Other dicarboxylic acids, such as glycolic acid and cis-pinonic acid were detected in only one sample

463 in which their LODs were exceeded (Supplemental Table S10). The possible reason for the low concentration  
 464 of glycolic acid might be that it can be formed as an oxidation product of biogenic isoprene (Liu et al., 2012).

### 465 3.6. Comparison of nitrogen-containing compounds and other VOCs at the altitudes of 50 m and 400 466 m

467 The aim of this study was to compare the composition of VOCs at the altitudes of 50 m and 400 m, separately.  
 468 Carbon WR-SPME Arrow unit with universal sorbent was used to collect a wide range of VOCs in the gas  
 469 phase. MCM-41-TP-ITEX and TENAX-GR-ITEX sampling systems were employed to collect gas and  
 470 particle phases.



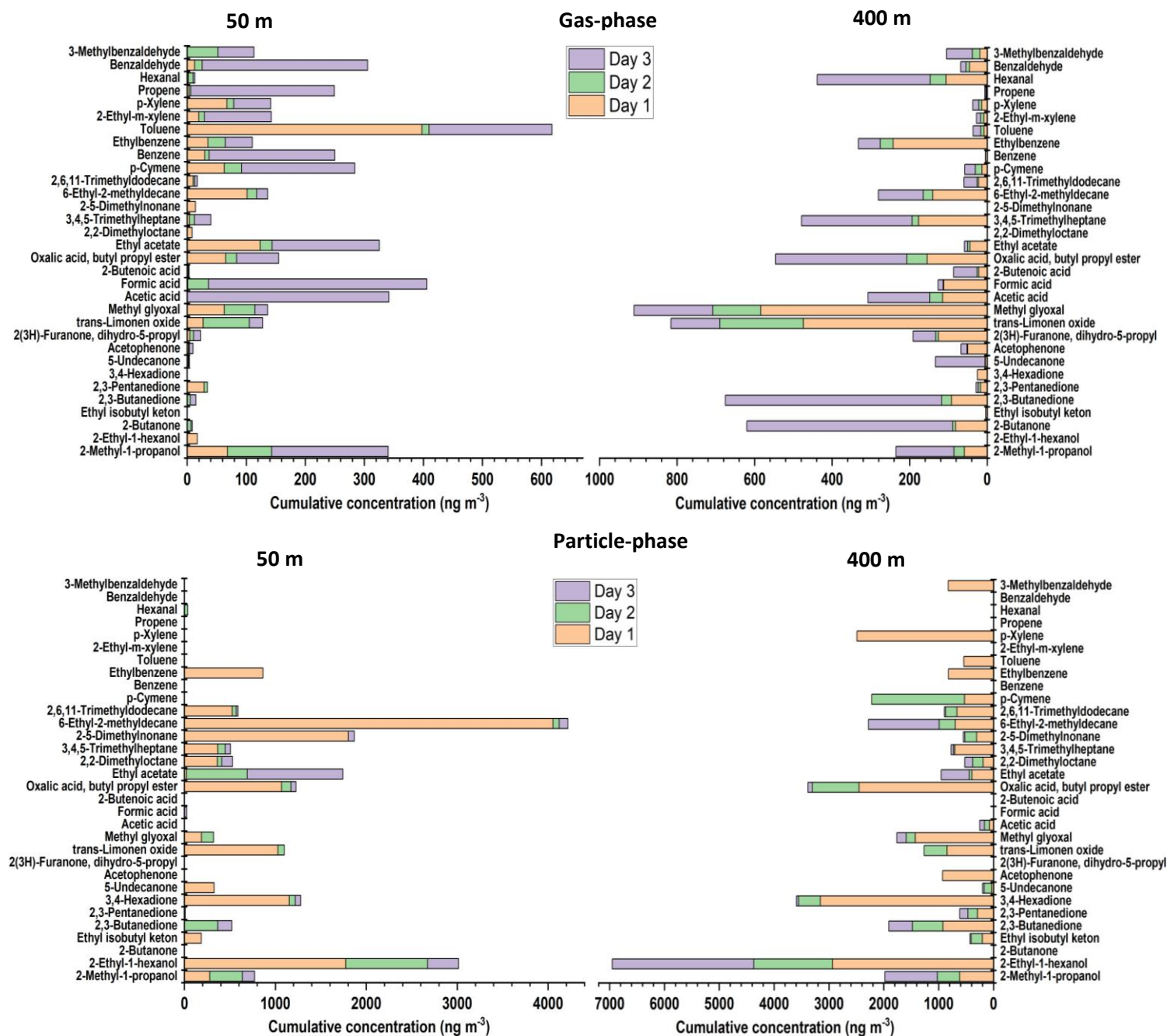
472

473 **Figure 4.** Concentrations of nitrogen-containing compounds in the gas-phase and in particle-phase at  
474 SMEAR II Station at altitudes 50 and 400 m for three days (8 to 10 October 2021). For the gas-phase samples  
475 were collected using Carbon WR-SPME Arrow sampling system, and the particle-phase samples were  
476 collected by MCM-41-TP-ITEX system. The concentrations of aerosol particle compounds were obtained  
477 via subtraction the results obtained by MCM-41-TP-ITEX from those obtained by Carbon WR-SPME Arrow  
478 with universal sorbent.

479 As can be seen from Fig. 4, the concentrations of amines that were emitted by biogenic sources, such as  
480 methylamine, dimethylamine, sec-butylamine, butanamine, pentanamine, hexylmethylamine, and  
481 heptylamine, were mostly found at higher concentrations at the lower altitude (50 m). The concentrations  
482 were decreased at higher altitude 400 m most probably due to the dilution (since the sources are on the  
483 ground) and reaction with hydroxyl radical (Kieloaho, 2017).

484 For nitrogen containing compounds, other than amines, imidazole was one of the compounds detected by our  
485 system. There have been a number of laboratory studies where imidazole has been reported to be the major  
486 product of glyoxal reaction with ammonium ions or primary amines on secondary organic aerosol. In  
487 addition, imidazoles can become a secondary product of the reaction of dicarbonyls with nitrogen containing  
488 compounds, therefore they might have potential to act as photosensitizers triggering secondary organic  
489 aerosol growth and are forming constituents of light absorbing brown carbon (De Haan et al., 2011; Dou et  
490 al., 2015; Teich et al., 2020). Imidazoles were detected mostly in the particle phase with concentrations up  
491 to 422 ng m<sup>-3</sup> at 50 m and 338 ng m<sup>-3</sup> at 400 m. Slightly lower concentrations were discovered in the gas  
492 phase with the values up to 58 ng m<sup>-3</sup> at the altitudes of 50 m, and 510 ng m<sup>-3</sup> at the altitude of 400 m.

493 Other nitrogen-containing gas phase compounds detected, such as formamide, 2-amino-1-propanol,  
494 ethylmethylcarbamate, and propenamide showed also the same pattern with higher concentrations at 400 m  
495 than at 50 m. These compounds were most probably transported by the wind from other areas and emitted by  
496 various sources, such as biomass burning, peatland, industries, and other anthropogenic sources (Pusfitasari  
497 et al., 2022).



499 **Figure 5.** Concentrations of non-nitrogenated VOC compounds in the gas-phase and in particle-phase at  
 500 SMEAR II Station at altitudes 50 and 400 m for three days (8 to 10 October 2022). The gas-phase samples  
 501 were collected using Carbon WR-SPME Arrow system, and particle-phase samples using TENAX-GR-ITEX  
 502 sampling systems. The concentrations of aerosol particle compounds were obtained via subtraction the results  
 503 obtained by TENAX-GR-ITEX from those obtained by Carbon WR-SPME Arrow with universal sorbent.

504 As can be seen from Fig. 5 gas-phase VOC compounds without nitrogen, such as trans-limonene oxide,  
505 methylglyoxal, hexanal and ketones have higher concentrations at the altitude of 400 m compared to 50 m.  
506 Whereas some acids, such as acetic acid and formic acid, ethyl acetate, and BTX (benzene, toluene, xylene)  
507 were mostly discovered at the altitude of 50 m. In the case of alcohols, they had comparable concentrations  
508 at both 50 and 400 m. In the particle phase, most of the compounds had higher concentrations at 400 m than  
509 at 50 m, except for some hydrocarbons (such as 2,5-dimethylnonane and 6-ethyl-2-methyldecane) that had  
510 high concentrations at 50 m.

511 Alcohols are a prevalent class of VOCs in the atmosphere and can be emitted by biogenic sources such as  
512 rain forest, and also from anthropogenic sources such as alcohol-gasoline blended fuel and industries  
513 (Nguyen et al., 2001; McGillen et al., 2017). Therefore, it is no wonder that in this study alcohol was found  
514 almost in all altitudes. The alcohol emission is becoming concern since it can react with Criegee intermediates  
515 (product of biogenic alkenes oxidized by ozone) to produce  $\alpha$ -alkoxyalkyl hydroperoxides (AAAHs) that can  
516 lead to the formation of secondary organic aerosols (Sahli, 1992; Bonn et al., 2004; McGillen et al., 2017).

517 In the gas phase samples, benzene, toluene, and p-xylene (BTX) were found mostly at the altitude of 50 m  
518 with the concentrations up to 219, 410, and 70  $\text{ng m}^{-3}$ , respectively. Since BTX can be emitted from the  
519 gasoline (major fuel of vehicles) and the samples were collected close to the parking area, the higher  
520 concentrations were found at lower altitude 50 m. This finding is comparable with the study conducted by  
521 Chen et al (2018) who measured the BTX concentrations between 100 and 300  $\text{ng m}^{-3}$  from forest canopy at  
522 the altitude between 20 and 26 m  $\text{m}^{-3}$ -(Chen et al., 2018; Yassaa et al., 2006). Toluene and p-xylene were  
523 also detected in the particle phase as VOCs may be adsorbed onto the surface of the particles (Dehghani et  
524 al., 2018; Kamens et al., 2011). The higher concentrations were detected at the altitude of 400 m with the  
525 concentrations of up to 539  $\text{ng m}^{-3}$  and 2475  $\text{ng m}^{-3}$  for toluene and p-xylene, respectively. BTX play an  
526 important role in the atmosphere since they have been recognized as important photochemical precursors for  
527 the secondary organic aerosol (Correa et al., 2012; Ng et al., 2007).

528 Aldehydes in the atmosphere are also of concern because of their heterogeneous reaction with acids affecting  
529 the particle growth (Jang and Kamens, 2001; Altshuller, 1993). In our study, some aldehydes, such as  
530 methylglyoxal, hexanal and benzaldehyde, were found both in the gas and particle phase at the altitude of  
531 400 m in higher concentrations than at the altitude of 50 m. At the altitude of 400 m, methylglyoxal was the  
532 most abundant aldehyde with the concentrations up to 580  $\text{ng m}^{-3}$  in the gas phase, and 1418  $\text{ng m}^{-3}$  in the  
533 particle phase. Ketones in aerosol particles have been associated with burning and non-burning forest, and it

534 represented up to 27 % of the current organic aerosol mass concentration (OM) (Takahama et al., 2011).  
535 Ketones were also found in this study at higher concentrations at high altitude 400 m in both gas phase and  
536 particle phase.

537 The last group of chemicals that was detected by our collection systems was small organic acids, and from  
538 these especially formic acid and acetic acid. Organic acids have an important role as chemical constituent in  
539 troposphere and they contribute with a large fraction (25 %) to the nonmethane hydrocarbons in the  
540 atmosphere. The organic acids contribute to the acidity of precipitation and cloud water (Khare et al., 1999).  
541 Acetic acid was found in both gas and particle phases at the altitudes of 50 and 400 m. However, the amount  
542 of both formic acid and acetic acid found in the gas phase was higher than that in the particle phase. These  
543 acids can originate from various sources such as vehicular emissions, ants, plants, soil, and biomass burning  
544 (Zhang et al., 2022).

### 545 **3.7. Evaluation of total particle numbers and black carbon at high altitudes. Portable CPC and BC** 546 **devices carried by aerial drone**

547 The particle number concentration and BC concentration were measured by using portable CPC and BC  
548 measurement devices carried by the drone. The BC concentration was measured at 880 nm wavelength (near  
549 IR), as at this wavelength BC has strong absorption and least interferences by other organic molecules  
550 (Dumka et al., 2010). The results were compared to those measured by the reference instruments at the  
551 SMEAR II Station. The correction factors to the same pressure level as described in section 2.8 were  
552 calculated with the values between 0.994 and 1.035 (Supplemental Table S1). Supplemental Figure S7 for  
553 CPC proves a correlation between the results obtained by our portable CPC and reference instrument, with  
554 direct linear close to 1 ( $R^2$  of 0.9564). Oppositely, linear correlation for BC was only 0.2492, indicating that  
555 there was no correlation between the reference instruments and our BC meter in the drone.

556 Our portable BC monitor in the drone gave higher concentration values than the reference one, located at 4  
557 m. The reasons for the differences could be caused by amplification factor that raised due to multiple  
558 scattering in quartz fiber matrix of the tape of the Aethalometer. The deposition of scattering material along  
559 with BC to the filter tape produced the “shadowing effect” causing the BC meter to show higher concentration  
560 values (Weingartner et al., 2003; Dumka et al., 2010). Alternatively, the differences can be explained by  
561 different measurement altitudes between the reference instrument (measured at 4 m) and BC monitor in the  
562 drone (up to 400 m). At lower altitude, living activities such as heating sauna and fuel burning from cars  
563 nearby the area might contribute to the results, while at higher altitudes BC long distance transport contributes

564 to the results as well (Meena et al., 2021). The atmospheric boundary layer height (ABLH) also plays an  
 565 important role to govern concentration of BC at high altitudes since it can affect pollutant aggregation,  
 566 transmission, wet deposition, and dry sedimentation (Meena et al., 2021). The boundary layer (BL) is the  
 567 lowest part of troposphere and connects the ground and the free atmosphere. The average boundary layer  
 568 height at Hyytiälä SMEAR II Station in autumn (October) was around 500 m (Sinclair et al., 2022),  
 569 explaining why we found higher BC concentration at high altitudes. For comparison, Table 3 shows the BC  
 570 mass concentrations measured at high altitudes in different areas.

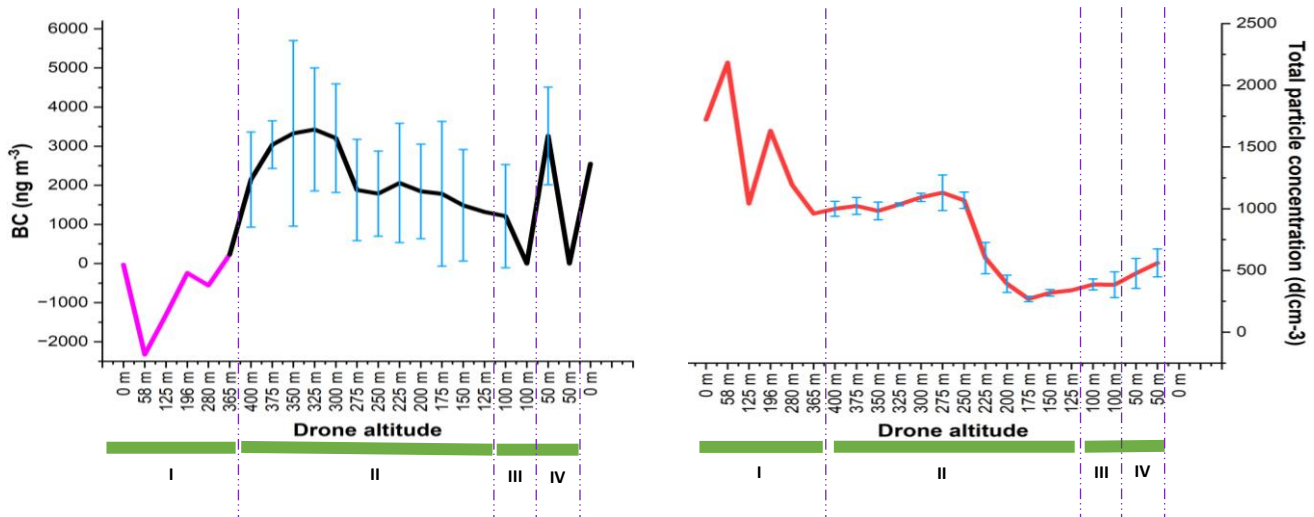
571 Table 3. Average BC concentrations observed at different locations.

Location	Altitude	Environment	Average BC concentration (ng m <sup>-3</sup> )	Reference
Hyytiälä, Finland	100 m	Boreal forest	2278±1188	This study
Hyytiälä, Finland	200 m	Boreal forest	2500±1497	This study
Hyytiälä, Finland	300 m	Boreal forest	3564±1648	This study
Hyytiälä, Finland	400 m	Boreal forest	3909±729	This study
<u>Hyytiälä, Finland</u>	<u>4 m</u>	<u>Boreal forest</u>	<u>320 – 1291 ± 337*</u>	<u>(Hyvärinen et al., 2011)</u>
Mahabaleswar, India	1378 m	Rural	2600 ± 260	(Meena et al., 2021)
Mountain Huang, China	1840 m	Rural	1663±919	(Pan et al., 2011)
Port Blair, India	73 m	Rural	2446±66	(Moorthy and Babu, 2006)
Sinhagad, India	1300 m	Rural	1500	(Safai et al., 2007)

572 \*320 ng m<sup>-3</sup> was the annual average, while 1291 ng m<sup>-3</sup> was the concentration average measured during pollution event in Autumn

573 Autumn average of BC pollution in Hyytiälä according to Hyvärinen *et al.* 2011 was about 1291 ng m<sup>-3</sup>,  
 574 while Hienola *et al* (2013) reported the October average was 550 ng m<sup>-3</sup> (Hyvärinen et al., 2011; Hienola et  
 575 al., 2013). However, those studies were conducted using reference instrument at low altitude, i.e. 4 meters  
 576 above the ground.





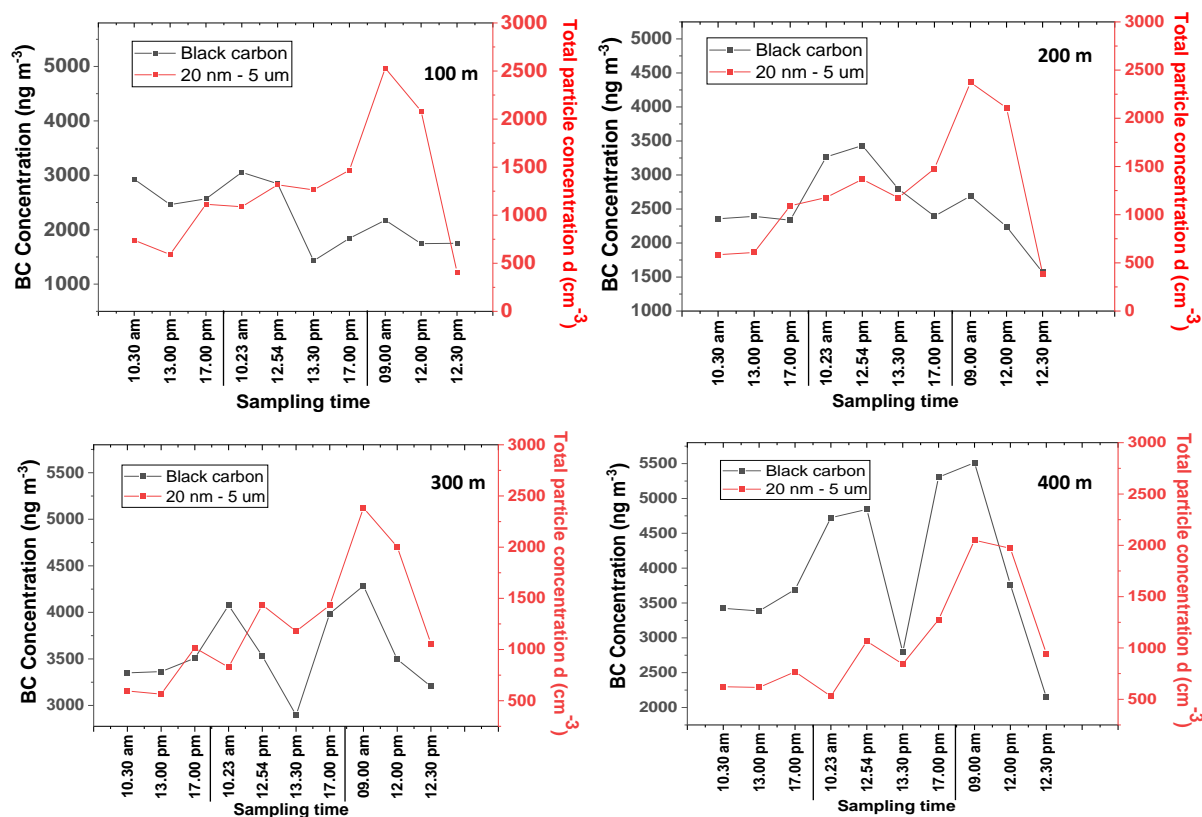
577

578 **Figure 6.** Evaluation of drone's vertical and horizontal movements. I = Drone is moving up with the speed  
 579 of  $2.5 \text{ ms}^{-1}$ . II= Drone is descending with the speed of  $1.25 \text{ ms}^{-1}$  to each altitude before staying for 30 s. III  
 580 and IV = Horizontal movement to 100 m far with the speed of  $5 \text{ ms}^{-1}$ .

581 The drone stability was evaluated during the vertical and horizontal movements (drone movement schematic  
 582 is showed in Supplemental Fig. S4). Figure 6 shows that the BC concentration and total particle numbers  
 583 were affected by the drone movements. Rapid ascending (area number I) affected both BC and CPC. BC  
 584 measurements showed negative values when the drone started warming up, take off, and then quickly moved  
 585 vertically with the speed of  $2.5 \text{ ms}^{-1}$ . These readings could be due to the temperature change on the BC sensor  
 586 when the drone ready to take off and drone fast ascending (Pan et al., 2011; Elomaa, 2022). Portable CPC  
 587 device gave also fluctuating data. Both BC device and CPC started to stabilize when approaching altitude of  
 588 365 m.

589 At the beginning of drone vertical movement at the altitude of 400 m, portable CPC gave more stable results  
 590 when the speed was decreased and when it was allowed to stabilize for 30 seconds (as can be seen in area  
 591 number II), resulting in smooth changes in the total particle numbers and some deviations at each altitude.  
 592 However, BC concentration varied also with high standard deviations at high altitude without any specific  
 593 movement, indicating that the drone movement influenced the portable BC device. Pan *et al* (2011) have  
 594 suggested that a large variation in the BC measurements could be caused by several factors such as boundary  
 595 layer stratification and turbulence. In addition, BC sensor was also very sensitive to change in temperature.  
 596 They observed that BC concentration could change quickly only after a short period of sunshine. Based on

597 the standard deviations' horizontal movements (area numbers III and IV), affected much less portable CPC,  
 598 compared to the portable BC.



599

600 **Figure 7.** Time series evaluation of CPC and black carbon at the heights of 100, 200, 300, and 400 m.  
 601 Sampling was conducted on October 9 (Day 1), 10 (Day 2), and 11 (Day 3), 2021. The values and point  
 602 averages are shown in Supplemental Table S11.

603 It can be seen from the results of Fig. 7 for three days measurements that BC and CPC had similar pattern at  
 604 all altitudes (100, 200, 300 and 400 m). The daily means of total particle numbers are found from  
 605 Supplemental Table S12. Although the concentrations at the altitude of 400 m seem to be slightly lower than  
 606 those detected at lower altitudes, the patterns of total particle number are similar at every altitude (Fig. 7),  
 607 most possible due to the limited anthropogenic activities near the sampling site. The potential mixing and the  
 608 particle formation in the atmosphere most likely influenced the total particle number detected. In addition,  
 609 particulates' long-range transport from different areas could also affect the total particle concentration in the  
 610 air (Casquero-Vera et al., 2020).

611 Figure 7 also demonstrates that diurnal pattern was different, revealing that the particle concentrations at  
612 different times of the day were influenced by different sources compared to BC. Almost at all altitudes, the  
613 diurnal variation for day 1 and day 2 included a late afternoon peak at 17:00. The particle concentrations  
614 increased significantly on the day 3, especially during the first and second samplings before the change to  
615 lower concentrations. The samplings for the first two days were carried out during the weekend without many  
616 activities that produce VOCs, opposite to Monday morning, when the normal working activities close to  
617 sampling area were going-on.

618 In contrast to the pattern of total particle numbers, the daily average of BC concentration during the  
619 measurement time period was increased at higher altitudes (Supplemental Table S12), indicating that BC  
620 pollutant was distributed from different areas. These trends agree well with the earlier studies (Tripathi et al.,  
621 2007). Figure 7 shows that BC diurnal pattern was similar with that of total particle numbers, except on day  
622 2 when BC concentration decreased significantly at 13.30, excluding the altitude of 200 m. However, BC  
623 concentration increased again at 17.00 most likely due to e.g. sauna heating and air mixing following long-  
624 range transport from different areas.

625 During the measurement time, BC at high altitudes 400 m and total particle numbers at all altitudes (100 –  
626 400 m) showed diurnal cycle with peak observed on Monday morning at 09:00 am, possible due to morning  
627 traffic, and/or to wind-driven pollution transport as suggested by previous studies (Bonasoni et al., 2010;  
628 Sandeep et al., 2022). The high BC concentration at high altitude, especially at 400 m, was mostly caused by  
629 long-range transport and the atmospheric boundary layer height as discussed earlier, and BC and also other  
630 particles contributed to the total particle numbers.

#### 631 **4. Conclusions**

632 An aerial drone carrying the reliable and versatile miniaturized air sampling systems SPME Arrow and ITEX  
633 and portable BC and CPC devices was successfully used for the collection of air samples. Up to 48 VOCs  
634 were detected in gas and particle phase samples, and their distribution at the altitude from 50 to 400 m was  
635 studied. Some differences between VOC compositions at the altitude 50 and 400 m could be explained by  
636 the different sources of the VOC emissions. The compounds that most probably originate from the same  
637 source had a linear correlation, as well as the compounds that were present both in gas and particle phase  
638 samples. The capability of ITEX sampler, furnished with filter accessory for the collection of gas phase  
639 samples, was evaluated by comparing it with SPME Arrow sampling resulting in high agreement especially  
640 for polar compounds with recoveries up to 99 %. In contrast, non-polar compounds gave low recoveries due

641 to the *like dissolve like* rule meaning that non-polar compounds might be adsorbed to the non-polar PTFE  
642 filter of the ITEX sampling system.

643 The portable CPC gave comparable results with those obtained by the conventional reference CPC  
644 instruments at the SMEAR II Station, opposite to the portable BC device that was affected by drone's vertical  
645 and horizontal movements. The total particle number and BC gave similar diurnal pattern, indicating that  
646 they were correlated. The pattern was observed during the weekend. The highest concentrations were found  
647 during times with human activities. The distribution was also similar to VOCs that were produced by  
648 anthropogenic sources and found in high altitude samples, since the wind most probably carried the VOCs  
649 from other sites. For spatial distribution pattern, BC concentrations were increased at higher altitudes due to  
650 long-range transport and the atmospheric boundary layer height. The total particle numbers, affected by the  
651 similar factors, varied more depending on the sources. This can be explained by the different VOCs that  
652 contributed to the particle formations, and the particle sizes measured by the portable CPC and BC monitors.

653 Overall, our study work described a drone equipped with miniaturized air sampling techniques, SPME Arrow  
654 and ITEX together with portable BC and CPC devices were for the collection of atmospheric VOCs and for  
655 the measurement of BC and total number of particles at high altitudes. To further improve the reliability of  
656 the results in the future, a portable BC monitor that includes a better electronic model and the possibility to  
657 adjust the device position in the drone are needed.

658 **Author contributions.** EDP, JR-J, JH, KH, MJ, TP and M-LR designed the experiments. EDP, AT, MS, JR-  
659 J carried out the experiments. EDP performed data interpretation and visualization. JR-J performed the  
660 statistical analysis. YW, JH, JK and KL were responsible for CPC and BC hardware, software and reference  
661 data. EDP, JR-J, KH, TP and M-LR prepared the manuscript with contributions from other co-authors.

662

663 **Declaration of competing Interest.** One of the (co-)authors is a member of the editorial board of  
664 *Atmospheric Chemistry and Physics*. The peer-review process was guided by an independent editor, and the  
665 authors have also no other competing interests to declare.

666 **Acknowledgments.** Financial support was provided by the Jane and Aatos Erkkö Foundation and Academy  
667 of Finland (ACCC flagship "Finnish Research Flagship" grant no. 337549). CTC Analytics AG (Zwingen,  
668 Switzerland) and BGB Analytik AG (Zürich, Switzerland) are thanked for the cooperation. Tapio Elomaa is  
669 also acknowledged for the fruitful discussion especially about Black Carbon (BC) and Condensation Particle

670 Counters (CPCs). In addition, we also thank the staff of the SMEAR II Station, Hyytiälä, for the valuable  
671 help.

## 672 **References**

- 673 Ahlberg, E., Falk, J., Eriksson, A., Holst, T., Brune, W. H., Kristensson, A., Roldin, P., and Svenningsson, B.:  
674 Secondary organic aerosol from VOC mixtures in an oxidation flow reactor, *Atmos. Environ.*, 161, 210–220,  
675 <https://doi.org/10.1016/j.atmosenv.2017.05.005>, 2017.
- 676 Almeida, J., Schobesberger, S., Kürten, A., Ortega, I. K., Kupiainen-Määttä, O., Praplan, A. P., Adamov, A.,  
677 Amorim, A., Bianchi, F., Breitenlechner, M., David, A., Dommen, J., Donahue, N. M., Downard, A., Dunne, E.,  
678 Duplissy, J., Ehrhart, S., Flagan, R. C., Franchin, A., Guida, R., Hakala, J., Hansel, A., Heinritzi, M., Henschel, H.,  
679 Jokinen, T., Junninen, H., Kajos, M., Kangasluoma, J., Keskinen, H., Kupc, A., Kurtén, T., Kvashin, A. N.,  
680 Laaksonen, A., Lehtipalo, K., Leiminger, M., Leppä, J., Loukonen, V., Makhmutov, V., Mathot, S., McGrath, M. J.,  
681 Nieminen, T., Olenius, T., Onnela, A., Petäjä, T., Riccobono, F., Riipinen, I., Rissanen, M., Rondo, L., Ruuskanen,  
682 T., Santos, F. D., Sarnela, N., Schallhart, S., Schnitzhofer, R., Seinfeld, J. H., Simon, M., Sipilä, M., Stozhkov, Y.,  
683 Stratmann, F., Tomé, A., Tröstl, J., Tsagkogeorgas, G., Vaattovaara, P., Viisanen, Y., Virtanen, A., Vrtala, A.,  
684 Wagner, P. E., Weingartner, E., Wex, H., Williamson, C., Wimmer, D., Ye, P., Yli-Juuti, T., Carslaw, K. S.,  
685 Kulmala, M., Curtius, J., Baltensperger, U., Worsnop, D. R., Vehkamäki, H., and Kirkby, J.: Molecular  
686 understanding of sulphuric acid-amine particle nucleation in the atmosphere, *Nature*, 502, 359–363,  
687 <https://doi.org/10.1038/nature12663>, 2013.
- 688 Altshuller, A. P.: Production of aldehydes as primary emissions and from secondary atmospheric reactions of alkenes  
689 and alkanes during the night and early morning hours, *Atmos. Environ. Part A, Gen. Top.*, 27, 21–32,  
690 [https://doi.org/10.1016/0960-1686\(93\)90067-9](https://doi.org/10.1016/0960-1686(93)90067-9), 1993.
- 691 Anenberg, S. C., Schwartz, J., Shindell, D., Amann, M., Faluvegi, G., Klimont, Z., Janssens-Maenhout, G., Pozzoli,  
692 L., van Dingenen, R., Vignati, E., Emberson, L., Muller, N. Z., Jason West, J., Williams, M., Demkine, V., Kevin  
693 Hicks, W., Kuylenstierna, J., Raes, F., and Ramanathan, V.: Global air quality and health co-benefits of mitigating  
694 near-term climate change through methane and black carbon emission controls, *Environ. Health Perspect.*, 120, 831–  
695 839, <https://doi.org/10.1289/ehp.1104301>, 2012.
- 696 Asbach, C., Schmitz, A., Schmidt, F., Monz, C., and Todea, A. M.: Intercomparison of a personal CPC and different  
697 conventional CPCs, *Aerosol Air Qual. Res.*, 17, 1132–1141, <https://doi.org/10.4209/aaqr.2016.10.0460>, 2017.
- 698 Bonasoni, P., Laj, P., Marinoni, A., Sprenger, M., Angelini, F., Arduini, J., Bonafè, U., Calzolari, F., Colombo, T.,  
699 Decesari, S., Di Biagio, C., Di Sarra, A. G., Evangelisti, F., Duchi, R., Facchini, M. C., Fuzzi, S., Gobbi, G. P.,  
700 Maione, M., Panday, A., Roccatò, F., Sellegri, K., Venzac, H., Verza, G. P., Villani, P., Vuillermoz, E., and  
701 Cristofanelli, P.: Atmospheric Brown Clouds in the Himalayas: First two years of continuous observations at the  
702 Nepal Climate Observatory-Pyramid (5079 m), *Atmos. Chem. Phys.*, 10, 7515–7531, <https://doi.org/10.5194/acp-10-7515-2010>, 2010.
- 704 Bonn, B., von Kuhlmann, R., and Lawrence, M. G.: High contribution of biogenic hydroperoxides to secondary  
705 organic aerosol formation, *Geophys. Res. Lett.*, 31, 1–4, <https://doi.org/10.1029/2003GL019172>, 2004.
- 706 Boylstein, R., Piacitelli, C., Grote, A., Kanwal, R., Kullman, G., and Kreiss, K.: Diacetyl emissions and airborne dust  
707 from butter flavorings used in microwave popcorn production, *J. Occup. Environ. Hyg.*, 3, 530–535,  
708 <https://doi.org/10.1080/15459620600909708>, 2006.
- 709 Brasseur, G. P., Orlando, J. J., and Tyndall, G. S.: *Atmospheric Chemistry and Global Change*, Oxford University  
710 Press, New York, 1999.
- 711 Buzorius, G., Rannik, Ü., Mäkelä, J. M., Vesala, T., and Kulmala, M.: Vertical aerosol particle fluxes measured by  
712 eddy covariance technique using condensational particle counter, *J. Aerosol Sci.*, 29, 157–171,  
713 [https://doi.org/10.1016/S0021-8502\(97\)00458-8](https://doi.org/10.1016/S0021-8502(97)00458-8), 1998.

714 Camredon, M., Aumont, B., Lee-Taylor, J., and Madronich, S.: The SOA/VOC/NO<sub>x</sub> system: an explicit model of  
715 secondary organic aerosol formation, *Atmos. Chem. Phys.*, 5599–5610 pp., 2007.

716 Carnerero, C., Pérez, N., Reche, C., Ealo, M., Titos, G., Lee, H. K., Eun, H. R., Park, Y. H., Dada, L., Paasonen, P.,  
717 Kerminen, V. M., Mantilla, E., Escudero, M., Gómez-Moreno, F. J., Alonso-Blanco, E., Coz, E., Saiz-Lopez, A.,  
718 Temime-Roussel, B., Marchand, N., Beddows, D. C. S., Harrison, R. M., Petäjä, T., Kulmala, M., Ahn, K. H.,  
719 Alastuey, A., and Querol, X.: Vertical and horizontal distribution of regional new particle formation events in  
720 Madrid, *Atmos. Chem. Phys.*, 18, 16601–16618, <https://doi.org/10.5194/acp-18-16601-2018>, 2018.

721 Casquero-Vera, J. A., Lyamani, H., Dada, L., Hakala, S., Paasonen, P., Román, R., Fraile, R., Petäjä, T., Olmo-  
722 Reyes, F. J., and Alados-Arboledas, L.: New particle formation at urban and high-altitude remote sites in the south-  
723 eastern Iberian Peninsula, *Atmos. Chem. Phys.*, 20, 14253–14271, <https://doi.org/10.5194/acp-20-14253-2020>, 2020.

724 Chen, J., Jiang, S., Liu, Y. R., Huang, T., Wang, C. Y., Miao, S. K., Wang, Z. Q., Zhang, Y., and Huang, W.:  
725 Interaction of oxalic acid with dimethylamine and its atmospheric implications, *RSC Adv.*, 7, 6374–6388,  
726 <https://doi.org/10.1039/c6ra27945g>, 2017.

727 Chen, J., Scircle, A., Black, O., Cizdziel, J. V., Watson, N., Wevill, D., and Zhou, Y.: On the use of multicopters for  
728 sampling and analysis of volatile organic compounds in the air by adsorption/thermal desorption GC-MS, *Air Qual.*  
729 *Atmos. Heal.*, 11, 835–842, <https://doi.org/10.1007/s11869-018-0588-y>, 2018.

730 Chen, T., Ge, Y., Liu, Y., and He, H.: N-nitration of secondary aliphatic amines in the particle phase, *Chemosphere*,  
731 293, 133639, <https://doi.org/10.1016/j.chemosphere.2022.133639>, 2022.

732 Correa, S. M., Arbilla, G., Marques, M. R. C., and Oliveira, K. M. P. G.: The impact of BTEX emissions from gas  
733 stations into the atmosphere, *Atmos. Pollut. Res.*, 3, 163–169, <https://doi.org/10.5094/APR.2012.016>, 2012.

734 Dehghani, M., Fazlzadeh, M., Sorooshian, A., Tabatabaee, H. R., Miri, M., Baghani, A. N., Delikhoon, M., Mahvi,  
735 A. H., and Rashidi, M.: Characteristics and health effects of BTEX in a hot spot for urban pollution, *Ecotoxicol.*  
736 *Environ. Saf.*, 155, 133–143, <https://doi.org/10.1016/j.ecoenv.2018.02.065>, 2018.

737 Dou, J., Lin, P., Kuang, B. Y., and Yu, J. Z.: Reactive oxygen species production mediated by humic-like substances  
738 in atmospheric aerosols: Enhancement effects by pyridine, imidazole, and their derivatives, *Environ. Sci. Technol.*,  
739 49, 6457–6465, <https://doi.org/10.1021/es5059378>, 2015.

740 Dumka, U. C., Moorthy, K. K., Kumar, R., Hegde, P., Sagar, R., Pant, P., Singh, N., and Babu, S. S.: Characteristics  
741 of aerosol black carbon mass concentration over a high altitude location in the Central Himalayas from multi-year  
742 measurements, *Atmos. Res.*, 96, 510–521, <https://doi.org/10.1016/j.atmosres.2009.12.010>, 2010.

743 Elomaa, T.: Mustan hiilen mittaus suodatinpohjaisilla sensoreilla, University of Helsinki, 2022.

744 Fermo, P., Artñano, B., De Gennaro, G., Pantaleo, A. M., Parente, A., Battaglia, F., Colicino, E., Di Tanna, G.,  
745 Goncalves da Silva Junior, A., Pereira, I. G., Garcia, G. S., Garcia Goncalves, L. M., Comite, V., and Miani, A.:  
746 Improving indoor air quality through an air purifier able to reduce aerosol particulate matter (PM) and volatile  
747 organic compounds (VOCs): Experimental results, *Environ. Res.*, 197, 1–8,  
748 <https://doi.org/10.1016/j.envres.2021.111131>, 2021.

749 Fu, P., Kawamura, K., Usukura, K., and Miura, K.: Dicarboxylic acids, ketocarboxylic acids and glyoxal in the  
750 marine aerosols collected during a round-the-world cruise, *Mar. Chem.*, 148, 22–32,  
751 <https://doi.org/10.1016/j.marchem.2012.11.002>, 2013.

752 Ge, X., Wexler, A. S., and Clegg, S. L.: Atmospheric amines - Part I. A review, *Atmos. Environ.*, 45, 524–546,  
753 <https://doi.org/10.1016/j.atmosenv.2010.10.012>, 2011.

754 De Haan, D. O., Hawkins, L. N., Kononenko, J. A., Turley, J. J., Corrigan, A. L., Tolbert, M. A., and Jimenez, J. L.:  
755 Formation of nitrogen-containing oligomers by methylglyoxal and amines in simulated evaporating cloud droplets,  
756 *Environ. Sci. Technol.*, 45, 984–991, <https://doi.org/10.1021/es102933x>, 2011.

757 Hari, P. and Kulmala, M.: Station for Measuring Ecosystem-Atmosphere Relations (SMEAR II), *Boreal Environ.*  
758 *Res.*, 10, 315–322, 2005.

759 Helin, A., Rönkkö, T., Parshintsev, J., Hartonen, K., Schilling, B., Läubli, T., and Riekkola, M. L.: Solid phase  
760 microextraction Arrow for the sampling of volatile amines in wastewater and atmosphere, *J. Chromatogr. A*, 1426,  
761 56–63, <https://doi.org/10.1016/j.chroma.2015.11.061>, 2015.

762 Hemmilä, M.: Chemical Characterisation of Boreal Forest Air with Chromatographic Techniques, University of  
763 Helsinki, Helsinki, 2020.

764 Hemmilä, M., Hellén, H., Virkkula, A., Makkonen, U., Praplan, A. P., Kontkanen, J., Ahonen, L., Kulmala, M., and  
765 Hakola, H.: Amines in boreal forest air at SMEAR II station in Finland, *Atmos. Chem. Phys.*, 18, 6367–6380,  
766 <https://doi.org/10.5194/acp-18-6367-2018>, 2018.

767 Hienola, A. I., Pietikäinen, J. P., Jacob, D., Pozdun, R., Petäjä, T., Hyvärinen, A. P., Sogacheva, L., Kerminen, V.  
768 M., Kulmala, M., and Laaksonen, A.: Black carbon concentration and deposition estimations in Finland by the  
769 regional aerosol-climate model REMO-HAM, *Atmos. Chem. Phys.*, 13, 4033–4055, [https://doi.org/10.5194/acp-13-](https://doi.org/10.5194/acp-13-4033-2013)  
770 4033-2013, 2013.

771 Hoeben, W. F. L. M., Beckers, F. J. C. M., Pemen, A. J. M., Van Heesch, E. J. M., and Kling, W. L.: Oxidative  
772 degradation of toluene and limonene in air by pulsed corona technology, *J. Phys. D. Appl. Phys.*, 45,  
773 <https://doi.org/10.1088/0022-3727/45/5/055202>, 2012.

774 Hyvärinen, A. P., Kolmonen, P., Kerminen, V. M., Virkkula, A., Leskinen, A., Komppula, M., Hatakka, J., Burkhart,  
775 J., Stohl, A., Aalto, P., Kulmala, M., Lehtinen, K. E. J., Viisanen, Y., and Lihavainen, H.: Aerosol black carbon at  
776 five background measurement sites over Finland, a gateway to the Arctic, *Atmos. Environ.*, 45, 4042–4050,  
777 <https://doi.org/10.1016/j.atmosenv.2011.04.026>, 2011.

778 Isidorov, V. A., Pirožnikow, E., Spirina, V. L., Vasyanin, A. N., Kulakova, S. A., Abdulmanova, I. F., and Zaitsev,  
779 A. A.: Emission of volatile organic compounds by plants on the floor of boreal and mid-latitude forests, *J. Atmos.*  
780 *Chem.*, 79, 153–166, <https://doi.org/10.1007/s10874-022-09434-3>, 2022.

781 Jacobson, M. Z.: Short-term effects of controlling fossil-fuel soot, biofuel soot and gases, and methane on climate,  
782 Arctic ice, and air pollution health, *J. Geophys. Res. Atmos.*, 115, <https://doi.org/10.1029/2009JD013795>, 2010.

783 Jang, M. and Kamens, R. M.: Atmospheric secondary aerosol formation by heterogeneous reactions of aldehydes in  
784 the presence of a sulfuric acid aerosol catalyst, *Environ. Sci. Technol.*, 35, 4758–4766,  
785 <https://doi.org/10.1021/es010790s>, 2001.

786 Junninen, H., Lauri, A., Keronen, P., Aalto, P., Hiltunen, V., Hari, P., and Kulmala, M.: Smart-SMEAR: On-line data  
787 exploration and visualization tool for SMEAR stations, *Boreal Environ. Res.*, 14, 447–457, 2009.

788 Kamens, R. M., Zhang, H., Chen, E. H., Zhou, Y., Parikh, H. M., Wilson, R. L., Galloway, K. E., and Rosen, E. P.:  
789 Secondary organic aerosol formation from toluene in an atmospheric hydrocarbon mixture: Water and particle seed  
790 effects, *Atmos. Environ.*, 45, 2324–2334, <https://doi.org/10.1016/j.atmosenv.2010.11.007>, 2011.

791 Kanakidou, M., Seinfeld, J. H., Pandis, S. N., Barnes, I., Dentener, F. J., Facchini, M. C., Van Dingenen, R., Ervens,  
792 B., Nenes, A., Nielsen, C. J., Swietlicki, E., Putaud, J. P., Balkanski, Y., Fuzzi, S., Horth, J., Moortgat, G. K.,  
793 Winterhalter, R., Myhre, C. E. L., Tsigaridis, K., Vignati, E., Stephanou, E. G., and Wilson, J.: Organic aerosol and  
794 global climate modelling: A review, *Atmos. Chem. Phys.*, 5, 1053–1123, <https://doi.org/10.5194/acp-5-1053-2005>,  
795 2005.

796 Kangasluoma, J. and Attoui, M.: Review of sub-3 nm condensation particle counters, calibrations, and cluster  
797 generation methods, *Aerosol Sci. Technol.*, 53, 1277–1310, <https://doi.org/10.1080/02786826.2019.1654084>, 2019.

798 Karlberg, A. -T, Magnusson, K., and Nilsson, U.: Air oxidation of d-limonene (the citrus solvent) creates potent  
799 allergens, *Contact Dermatitis*, 26, 332–340, <https://doi.org/10.1111/j.1600-0536.1992.tb00129.x>, 1992.

800 Kawamura, K. and Sakaguchi, F.: Acids Were Detected in the Sample3S ). With a Concentration Range of, North,  
801 104, 3501–3509, 1999.

802 Khare, P., Kumar, N., Kumari, K. M., and Srivastava, S. S.: Atmospheric formic acid and acetic acids : an overview,  
803 Rev. Geophys., 227–248, 1999.

804 Kieloaho, A.: Alkyl Amines in Boreal Forest and Urban Area, 2017.

805 Kim, H., Park, Y., Kim, W., and Eun, H.: Vertical Aerosol Distribution and Flux Measurement in the Planetary  
806 Boundary Layer Using Drone, 14, 35–40, 2018.

807 Kim, S. H., Kirakosyan, A., Choi, J., and Kim, J. H.: Detection of volatile organic compounds (VOCs), aliphatic  
808 amines, using highly fluorescent organic-inorganic hybrid perovskite nanoparticles, Dye. Pigment., 147, 1–5,  
809 <https://doi.org/10.1016/j.dyepig.2017.07.066>, 2017.

810 Kim, S. J., Lee, J. Y., Choi, Y. S., Sung, J. M., and Jang, H. W.: Comparison of different types of SPME arrow  
811 sorbents to analyze volatile compounds in *cirsium setidens nakai*, Foods, 9, <https://doi.org/10.3390/foods9060785>,  
812 2020.

813 Kivekäs, N., Sun, J., Zhan, M., Kerminen, V., Hyvärinen, A., Komppula, M., Viisanen, Y., Hong, N., Zhang, Y.,  
814 Kulmala, M., Zhang, X., and Lihavainen, H.: Long term particle size distribution measurements at Mount Waliguan,  
815 a high-altitude site in inland China, Atmos. Chem. Phys, 5461–5474 pp., 2009.

816 Kopperi, M., Ruiz-Jiménez, J., Hukkinen, J. I., and Riekkola, M. L.: New way to quantify multiple steroidal  
817 compounds in wastewater by comprehensive two-dimensional gas chromatography-time-of-flight mass spectrometry,  
818 Anal. Chim. Acta, 761, 217–226, <https://doi.org/10.1016/j.aca.2012.11.059>, 2013.

819 Kristensen, K., Bilde, M., Aalto, P. P., Petäjä, T., and Glasius, M.: Denuder/filter sampling of organic acids and  
820 organosulfates at urban and boreal forest sites: Gas/particle distribution and possible sampling artifacts, Atmos.  
821 Environ., 130, 36–53, <https://doi.org/10.1016/j.atmosenv.2015.10.046>, 2016.

822 Krueve, A.: Influence of mobile phase, source parameters and source type on electrospray ionization efficiency in  
823 negative ion mode, J. Mass Spectrom., 51, 596–601, <https://doi.org/10.1002/jms.3790>, 2016.

824 Kulmala, M., Kontkanen, J., Junninen, H., Lehtipalo, K., Manninen, H. E., Nieminen, T., Petäjä, T., Sipilä, M.,  
825 Schobesberger, S., Rantala, P., Franchin, A., Jokinen, T., Järvinen, E., Äijälä, M., Kangasluoma, J., Hakala, J., Aalto,  
826 P. P., Paasonen, P., Mikkilä, J., Vanhanen, J., Aalto, J., Hakola, H., Makkonen, U., Ruuskanen, T., Mauldin, R. L.,  
827 Duplissy, J., Vehkamäki, H., Bäck, J., Kortelainen, A., Riipinen, I., Kurtén, T., Johnston, M. V., Smith, J. N., Ehn,  
828 M., Mentel, T. F., Lehtinen, K. E. J., Laaksonen, A., Kerminen, V. M., and Worsnop, D. R.: Direct observations of  
829 atmospheric aerosol nucleation, Science (80-. ), 339, 943–946, <https://doi.org/10.1126/science.1227385>, 2013.

830 Kulmala, M., Petäjä, T., Ehn, M., Thornton, J., Sipilä, M., Worsnop, D. R., and Kerminen, V. M.: Chemistry of  
831 atmospheric nucleation: On the recent advances on precursor characterization and atmospheric cluster composition in  
832 connection with atmospheric new particle formation, Annu. Rev. Phys. Chem., 65, 21–37,  
833 <https://doi.org/10.1146/annurev-physchem-040412-110014>, 2014.

834 Kumar, R., Barth, M. C., Nair, V. S., Pfister, G. G., Suresh Babu, S., Satheesh, S. K., Krishna Moorthy, K.,  
835 Carmichael, G. R., Lu, Z., and Streets, D. G.: Sources of black carbon aerosols in South Asia and surrounding  
836 regions during the Integrated Campaign for Aerosols, Gases and Radiation Budget (ICARB), Atmos. Chem. Phys.,  
837 15, 5415–5428, <https://doi.org/10.5194/acp-15-5415-2015>, 2015.

838 Lan, H., Holopainen, J., Hartonen, K., Jussila, M., Ritala, M., and Riekkola, M. L.: Fully Automated Online  
839 Dynamic In-Tube Extraction for Continuous Sampling of Volatile Organic Compounds in Air, Anal. Chem., 91,  
840 8507–8515, <https://doi.org/10.1021/acs.analchem.9b01668>, 2019a.

841 Lan, H., Zhang, W., Smått, J.-H., Koivula, R. T., Hartonen, K., and Riekkola, M.-L.: Selective extraction of aliphatic  
842 amines by functionalized mesoporous silica-coated solid phase microextraction Arrow, Microchim. Acta, 186, 412,



843 <https://doi.org/10.1007/s00604-019-3523-5>, 2019b.

844 Lan, H., Hartonen, K., and Riekkola, M. L.: Miniaturised air sampling techniques for analysis of volatile organic  
845 compounds in air, *TrAC - Trends Anal. Chem.*, 126, 115873, <https://doi.org/10.1016/j.trac.2020.115873>, 2020.

846 Lan, H., Ruiz-Jimenez, J., Leleev, Y., Demaria, G., Jussila, M., Hartonen, K., and Riekkola, M.-L.: Quantitative  
847 analysis and spatial and temporal distribution of volatile organic compounds in atmospheric air by utilizing drone  
848 with miniaturized samplers, *Chemosphere*, 282, 131024, <https://doi.org/10.1016/j.chemosphere.2021.131024>, 2021.

849 Liu, Y., Monod, A., Tritscher, T., Praplan, A. P., Decarlo, P. F., Temime-Roussel, B., Quivet, E., Marchand, N.,  
850 Dommen, J., and Baltensperger, U.: Aqueous phase processing of secondary organic aerosol from isoprene  
851 photooxidation, *Atmos. Chem. Phys.*, 12, 5879–5895, <https://doi.org/10.5194/acp-12-5879-2012>, 2012.

852 McGillen, M. R., Curchod, B. F. E., Chhantyal-Pun, R., Beames, J. M., Watson, N., Khan, M. A. H., McMahan, L.,  
853 Shallcross, D. E., and Orr-Ewing, A. J.: Criegee Intermediate-Alcohol Reactions, A Potential Source of  
854 Functionalized Hydroperoxides in the Atmosphere, *ACS Earth Sp. Chem.*, 1, 664–672,  
855 <https://doi.org/10.1021/acsearthspacechem.7b00108>, 2017.

856 McMurry, P. H.: The history of condensation nucleus counters, *Aerosol Sci. Technol.*, 33, 297–322,  
857 <https://doi.org/10.1080/02786820050121512>, 2000.

858 Meena, G. S., Mukherjee, S., Buchunde, P., Safai, P. D., Singla, V., Aslam, M. Y., Sonbawne, S. M., Made, R.,  
859 Anand, V., Dani, K. K., and Pandithurai, G.: Seasonal variability and source apportionment of black carbon over a  
860 rural high-altitude and an urban site in western India, *Atmos. Pollut. Res.*, 12, 32–45,  
861 <https://doi.org/10.1016/j.apr.2020.10.006>, 2021.

862 Moorthy, K. K. and Babu, S. S.: Aerosol black carbon over Bay of Bengal observed from an island location, Port  
863 Blair: Temporal features and long-range transport, *J. Geophys. Res. Atmos.*, 111, 1–10,  
864 <https://doi.org/10.1029/2005JD006855>, 2006.

865 Ng, N. L., Kroll, J. H., Chan, A. W. H., Chhabra, P. S., Flagan, R., and Seinfeld, J. H.: Pytannia Vzaiemodii  
866 Partyzaniv Z Chastynamy Chervonoi Armii Pid Chas Vyzvolennia Pravoberezhnoi Ukrainy V Radians’Kii  
867 Istoriohrafii., *Atmos. Chem. Phys.*, 7, 3909–3922, 2007.

868 Nguyen, H. T. H., Takenaka, N., Bandow, H., Maeda, Y., De Oliva, S. T., Botelho, M. M. F., and Tavares, T. M.:  
869 Atmospheric alcohols and aldehydes concentrations measured in Osaka, Japan and in Sao Paulo, Brazil, *Atmos.*  
870 *Environ.*, 35, 3075–3083, [https://doi.org/10.1016/S1352-2310\(01\)00136-4](https://doi.org/10.1016/S1352-2310(01)00136-4), 2001.

871 Oh, H. J., Ma, Y., and Kim, J.: Human inhalation exposure to aerosol and health effect: Aerosol monitoring and  
872 modelling regional deposited doses, *Int. J. Environ. Res. Public Health*, 17, 1–2,  
873 <https://doi.org/10.3390/ijerph17061923>, 2020.

874 Olsen, R., Thorud, S., Hershon, M., Øvrebø, S., Lundanes, E., Greibrokk, T., Ellingsen, D. G., Thomassen, Y., and  
875 Molander, P.: Determination of the dialdehyde glyoxal in workroom air - Development of personal sampling  
876 methodology, *J. Environ. Monit.*, 9, 687–694, <https://doi.org/10.1039/b700105n>, 2007.

877 Pan, X. L., Kanaya, Y., Wang, Z. F., Liu, Y., Pochanart, P., Akimoto, H., Sun, Y. L., Dong, H. B., Li, J., Irie, H., and  
878 Takigawa, M.: Correlation of black carbon aerosol and carbon monoxide in the high-altitude environment of Mt.  
879 Huang in Eastern China, *Atmos. Chem. Phys.*, 11, 9735–9747, <https://doi.org/10.5194/acp-11-9735-2011>, 2011.

880 Parshintsev, J., Ruiz-Jimenez, J., Petäjä, T., Hartonen, K., Kulmala, M., and Riekkola, M. L.: Comparison of quartz  
881 and Teflon filters for simultaneous collection of size-separated ultrafine aerosol particles and gas-phase zero samples,  
882 *Anal. Bioanal. Chem.*, 400, 3527–3535, <https://doi.org/10.1007/s00216-011-5041-0>, 2011.

883 Parsons, G. E., Buckton, G., and Chatham B’, S. M.: The use of surface energy and polarity determinations to  
884 predict physical stability of non-polar, non-aqueous suspensions, *International Journal of Pharmaceutics*, 163–170  
885 pp., 1992.

886 Peng, L., Li, Z., Zhang, G., Bi, X., Hu, W., Tang, M., Wang, X., Peng, P., and Sheng, G.: A review of measurement  
887 techniques for aerosol effective density, *Sci. Total Environ.*, 778, 146248,  
888 <https://doi.org/10.1016/j.scitotenv.2021.146248>, 2021.

889 Perez, J. E., Kumar, M., Francisco, J. S., and Sinha, A.: Oxygenate-Induced Tuning of Aldehyde-Amine Reactivity  
890 and Its Atmospheric Implications, *J. Phys. Chem. A*, 121, 1022–1031, <https://doi.org/10.1021/acs.jpca.6b10845>,  
891 2017.

892 Petäjä, T., Rannik, Ü., Buzorius, G., Aalto, P., Vesala, T., and Kulmala, M.: Deposition Velocities of Ultrafine  
893 Particles Into Scots Pine Forest During Nucleation Events, *J. Aerosol Sci.*, 32, 143–144,  
894 [https://doi.org/10.1016/s0021-8502\(21\)00068-9](https://doi.org/10.1016/s0021-8502(21)00068-9), 2001.

895 Petäjä, T., Laakso, L., Grönholm, T., Launiainen, S., Evele-Peltoniemi, I., Virkkula, A., Leskinen, A., Backman, J.,  
896 Manninen, H. E., Sipilä, M., Haapanala, S., Hämeri, K., Vanhala, E., Tuomi, T., Paatero, J., Aurela, M., Hakola, H.,  
897 Makkonen, U., Hellén, H., Hillamo, R., Vira, J., Prank, M., Sofiev, M., Siitari-Kauppi, M., Laaksonen, A., Lehtinen,  
898 K. E. J., Kulmala, M., Viisanen, Y., and Kerminen, V. M.: In-situ observations of Eyjafjallajökull ash particles by  
899 hot-air balloon, *Atmos. Environ.*, 48, 104–112, <https://doi.org/10.1016/j.atmosenv.2011.08.046>, 2012.

900 Pusfitasari, E. D., Ruiz-Jimenez, J., Heiskanen, I., Jussila, M., Hartonen, K., and Riekkola, M.-L.: Aerial drone  
901 furnished with miniaturized versatile air sampling systems for selective collection of nitrogen containing compounds  
902 in boreal forest, *Sci. Total Environ.*, 808, 152011, <https://doi.org/10.1016/J.SCITOTENV.2021.152011>, 2022.

903 Rajesh, T. A. and Ramachandran, S.: Black carbon aerosols over urban and high altitude remote regions:  
904 Characteristics and radiative implications, *Atmos. Environ.*, 194, 110–122,  
905 <https://doi.org/10.1016/j.atmosenv.2018.09.023>, 2018.

906 Rinaldi, M., Decesari, S., Carbone, C., Finessi, E., Fuzzi, S., Ceburnis, D., O’Dowd, C. D., Sciare, J., Burrows, J. P.,  
907 Vrekoussis, M., Ervens, B., Tsigaridis, K., and Facchini, M. C.: Evidence of a natural marine source of oxalic acid  
908 and a possible link to glyoxal, *J. Geophys. Res. Atmos.*, 116, 1–12, <https://doi.org/10.1029/2011JD015659>, 2011.

909 Rosado-Reyes, C. M. and Francisco, J. S.: Atmospheric oxidation pathways of acetic acid, *J. Phys. Chem. A*, 110,  
910 4419–4433, <https://doi.org/10.1021/jp0567974>, 2006.

911 Ruiz-Jimenez, J., Zanca, N., Lan, H., Jussila, M., Hartonen, K., and Riekkola, M. L.: Aerial drone as a carrier for  
912 miniaturized air sampling systems, *J. Chromatogr. A*, 1597, 202–208, <https://doi.org/10.1016/j.chroma.2019.04.009>,  
913 2019.

914 Safai, P. D., Kewat, S., Praveen, P. S., Rao, P. S. P., Momin, G. A., Ali, K., and Devara, P. C. S.: Seasonal variation  
915 of black carbon aerosols over a tropical urban city of Pune, India, *Atmos. Environ.*, 41, 2699–2709,  
916 <https://doi.org/10.1016/j.atmosenv.2006.11.044>, 2007.

917 Sahli, A.: X ; H ; X, 1009–1012, 1992.

918 Sandeep, K., Panicker, A. S., Gautam, A. S., Beig, G., Gandhi, N., S, S., Shankar, R., and Nainwal, H. C.: Black  
919 carbon over a high altitude Central Himalayan Glacier: Variability, transport, and radiative impacts, *Environ. Res.*,  
920 204, <https://doi.org/10.1016/j.envres.2021.112017>, 2022.

921 Sato, K., Ikemori, F., Ramasamy, S., Fushimi, A., Kumagai, K., Iijima, A., and Morino, Y.: Four- and five-carbon  
922 dicarboxylic acids present in secondary organic aerosol produced from anthropogenic and biogenic volatile organic  
923 compounds, *Atmosphere (Basel)*, 12, <https://doi.org/10.3390/atmos12121703>, 2021.

924 Sinclair, V. A., Ritvanen, J., Urbancic, G., Statnaia, I., Batrak, Y., Moisseev, D., and Kurppa, M.: Boundary-layer  
925 height and surface stability at Hyytiälä, Finland, in ERA5 and observations, *Atmos. Meas. Tech.*, 15, 3075–3103,  
926 <https://doi.org/10.5194/amt-15-3075-2022>, 2022.

927 Takahama, S., Schwartz, R. E., Russell, L. M., MacDonald, A. M., Sharma, S., and Leaitch, W. R.: Organic  
928 functional groups in aerosol particles from burning and non-burning forest emissions at a high-elevation mountain

929 site, *Atmos. Chem. Phys.*, 11, 6367–6386, <https://doi.org/10.5194/acp-11-6367-2011>, 2011.

930 Teich, M., Schmidpott, M., van Pinxteren, D., Chen, J., and Herrmann, H.: Separation and quantification of  
931 imidazoles in atmospheric particles using LC–Orbitrap-MS, *J. Sep. Sci.*, 43, 577–589,  
932 <https://doi.org/10.1002/jssc.201900689>, 2020.

933 Tripathi, S. N., Srivastava, A. K., Dey, S., Satheesh, S. K., and Krishnamoorthy, K.: The vertical profile of  
934 atmospheric heating rate of black carbon aerosols at Kanpur in northern India, *Atmos. Environ.*, 41, 6909–6915,  
935 <https://doi.org/10.1016/j.atmosenv.2007.06.032>, 2007.

936 Weingartner, E., Saathoff, H., Schnaiter, M., Streit, N., Bitnar, B., and Baltensperger, U.: Absorption of light by soot  
937 particles: Determination of the absorption coefficient by means of aethalometers, *J. Aerosol Sci.*, 34, 1445–1463,  
938 [https://doi.org/10.1016/S0021-8502\(03\)00359-8](https://doi.org/10.1016/S0021-8502(03)00359-8), 2003.

939 Wen, L., Schaefer, T., He, L., Zhang, Y., Sun, X., Ventura, O. N., and Herrmann, H.: T- And pH-Dependent Kinetics  
940 of the Reactions of  $\cdot\text{OH}(\text{aq})$  with Glutaric and Adipic Acid for Atmospheric Aqueous-Phase Chemistry, *ACS Earth  
941 Sp. Chem.*, 5, 1854–1864, <https://doi.org/10.1021/acsearthspacechem.1c00163>, 2021.

942 Yassaa, N., Brancaloni, E., Frattoni, M., and Ciccioli, P.: Isomeric analysis of BTEXs in the atmosphere using  $\beta$ -  
943 cyclodextrin capillary chromatography coupled with thermal desorption and mass spectrometry, *Chemosphere*, 63,  
944 502–508, <https://doi.org/10.1016/j.chemosphere.2005.08.010>, 2006.

945 Youn, J.-S., Crosbie, E.S. B., Maudlin, L. C., Wang, Z., and Sorooshian, A.: Dimethylamine as a major alkyl amine  
946 species in particles and cloud water: Observations in semi-arid and coastal regions, *Atmos. Environ.*, 122, 250–258,  
947 <https://doi.org/doi:10.1016/j.atmosenv.2015.09.061>, 2015.

948 Yu, K., Mitch, W. A., and Dai, N.: Nitrosamines and Nitramines in Amine-Based Carbon Dioxide Capture Systems:  
949 Fundamentals, Engineering Implications, and Knowledge Gaps, *Environ. Sci. Technol.*, 51, 11522–11536,  
950 <https://doi.org/10.1021/acs.est.7b02597>, 2017.

951 Zahardis, J., Geddes, S., and Petrucci, G. A.: The ozonolysis of primary aliphatic amines in fine particles, *Atmos.  
952 Chem. Phys.*, 8, 1181–1194, <https://doi.org/10.5194/acp-8-1181-2008>, 2008.

953 Zhang, R., Shen, J., Xie, H.-B., Chen, J., and Elm, J.: The role of organic acids in new particle formation from  
954 methanesulfonic acid and methylamine, *Atmos. Chem. Phys.*, 22, 2639–2650, [https://doi.org/doi.org/10.5194/acp-22-  
955 2639-2022](https://doi.org/doi.org/10.5194/acp-22-2639-2022), 2022.

956 Zhang, Y., Wang, X., Wen, S., Herrmann, H., Yang, W., Huang, X., Zhang, Z., Huang, Z., He, Q., and George, C.:  
957 On-road vehicle emissions of glyoxal and methylglyoxal from tunnel tests in urban Guangzhou, China, *Atmos.  
958 Environ.*, 127, 55–60, <https://doi.org/10.1016/j.atmosenv.2015.12.017>, 2016.

959 Zhao, Y. L., Garrison, S. L., Gonzalez, C., Thweatt, W. D., and Marquez, M.: N-nitrosation of amines by NO<sub>2</sub> and  
960 NO: A theoretical study, *J. Phys. Chem. A*, 111, 2200–2205, <https://doi.org/10.1021/jp0677703>, 2007.

961 Ziemann, P. J. and Atkinson, R.: Kinetics, products, and mechanisms of secondary organic aerosol formation, *Chem.  
962 Soc. Rev.*, 41, 6582–6605, <https://doi.org/10.1039/c2cs35122f>, 2012.

963